Versicolorin A, a precursor in aflatoxins biosynthesis, is a food contaminant toxic for human intestinal cells

Thierry Gauthier, Carolina Duarte-Hospital, Julien Vignard, Elisa Boutet-Robinet, Michael Sulyok, Selma Snini, Imourana Alassane-Kpembi, Yannick Lippi, Sylvie Puel, Isabelle P. Oswald, et al.

Environment International 137 (2020) 105568

Contents lists available at ScienceDirect

Environment International

journal homepage: www.elsevier.com/locate/envint

Versicolorin A, a precursor in aflatoxins biosynthesis, is a food contaminant toxic for human intestinal cells

Thierry Gauthier[a,*], Carolina Duarte-Hospital[a], Julien Vignard[a], Elisa Boutet-Robinet[a], Michael Sulyok[b], Selma P. Snini[a,1], Imourana Alassane-Kpembi[a,2], Yannick Lippi[a], Sylvie Puel[a], Isabelle P. Oswald[a], Olivier Puel[a,*]

[a] Toxalim (Research Centre in Food Toxicology), Université de Toulouse, INRA, ENVT, INP-Purpan, UPS, Toulouse, France
[b] Institute of Bioanalytics and Agro-Metabolomics, Department IFA-Tulln, University of Natural Resources and Life Sciences Vienna (BOKU), A-3430 Tulln, Austria

ARTICLE INFO

Handling Editor: Adrian Covaci

Keywords:
Mycotoxins
Versicolorin A
Aflatoxin B1
Human colon cells
Genotoxicity
Cytotoxicity

ABSTRACT

Aflatoxin B_1 (AFB_1) is the most potent carcinogen among mycotoxins. Its biosynthesis involves the formation of versicolorin A (VerA), whose chemical structure shares many features with AFB_1. Our data revealed significant levels of VerA in foodstuff from Central Asia and Africa. Given this emerging food risk, it was of prime interest to compare the toxic effects of the two mycotoxins against cells originating from the intestinal tract. We used human colon cell lines (Caco-2, HCT116) to investigate the cytotoxic process induced by the two mycotoxins. Contrary to AFB_1, a low dose of VerA (1 μM) disturbed the expression level of thousands of genes (18 002 genes). We show that the cytotoxic effects of low doses of VerA (1–20 μM) were stronger than the same low doses of AFB_1 in both Caco-2 and HCT116 cell lines. In Caco-2 cells, VerA induced DNA strand breaks that led to apoptosis and reduced DNA replication of dividing cells, consequently inhibiting cell proliferation. Although VerA was able to induce the p53 signaling pathway in p53 wild-type HCT116 cells, its toxicity process did not mainly rely on p53 expression since similar cytotoxic effects were also observed in HCT116 cells that do not express p53. In conclusion, this study provides evidence of the risk of food contamination by VerA and shed light on its toxicological effect on human colon cells.

1. Introduction

The presence of mold in the environment is a source of contamination for foodstuff and hence mycotoxins are natural contaminants found in human food and animal feed (Cano et al., 2016). Among them, aflatoxins are considered the most toxic mycotoxin family. They are fungal secondary metabolites principally produced by *Aspergillus flavus* and *A. parasiticus* in tropical regions where the hot wet climate favors their development. They contaminate many foodstuffs, particularly groundnuts, corn, rice, sorghum, milk and food oils (Strosnider et al., 2006; Williams et al., 2004). With global warming, climate change scenarios for European regions tend to favor the production of aflatoxins in corn crops (Bailly et al., 2018; Battilani et al., 2016). Among aflatoxins, aflatoxin B_1 (AFB_1) is the most potent natural liver carcinogen (Kew, 2013), classified in group 1 (high level carcinogenic potential) by IARC (International Agency for Research on Cancer). AFB_1 has been shown to have hepatocarcinogenic, immunotoxic and teratogenic properties (International Agency for Research on Cancer and Weltgesundheitsorganisation, 2012).

Versicolorin A (VerA) is the first intermediate metabolite in the AFB_1 biosynthetic pathway bearing a furofuran ring. A previous study (Lee et al., 1976) demonstrated that 46% of VerA was converted to AFB_1 in *A. parasiticus*. This metabolite was detected in corn grain at higher concentrations than AFB_1, with a VerA/AFB_1 ratio exceeding ten (Zhang et al., 2018). The molecular structure of VerA is close to that of AFB_1 (Fig. S1). Notably, the double bond at the 12, 13 -position of the terminal furan ring of VerA corresponds to the activation site of AFB_1 (Mori et al., 1985). Metabolization of AFB_1 via cytochrome P450 (CYP450) results in its reaction product, AFB_1-8,9- epoxide, that then forms promutagenic DNA adducts (Bennett et al., 1981). The toxicity process of AFB_1 has been widely documented in several kinds of cells including hepatocytes (Liao et al., 2014; Liu and Wang, 2016; Yang

* Corresponding authors at: INRAE, UMR 1331 TOXALIM, 180, Chemin de Tournefeuille, F-31027 Toulouse, France.
E-mail addresses: thierry.gauthier@inrae.fr (T. Gauthier), olivier.puel@inrae.fr (O. Puel).
[1] Present address: Laboratoire de Génie Chimique, Université de Toulouse, CNRS, INPT, UPS, 31326 Toulouse, France.
[2] Present address: Department of Veterinary Biomedicine, Faculty of Veterinary Medicine, Université de Montréal, 3200 rue Sicotte, Saint-Hyacinthe, Québec J2S 2M2, Canada.

https://doi.org/10.1016/j.envint.2020.105568
Received 25 September 2019; Received in revised form 16 January 2020; Accepted 9 February 2020
Available online 24 February 2020

et al., 2016), intestinal cells (Kim et al., 2016; Yin et al., 2016; Zhang et al., 2015), spleen cells (Zhu et al., 2017), cardiomyocytes (Ge et al., 2017) and macrophages (Bianco et al., 2012). Briefly, exposure to AFB_1 has been shown to lead to DNA damage and, depending on the type of cells, to cell cycle arrest and/or apoptosis. Much less information is available on the cytotoxic process induced by VerA. One early study showed that VerA was cytotoxic for rat and mouse hepatocytes (Mori et al., 1984). More recently, cytotoxic and genotoxic effects of VerA were first observed in A549 lung cells (Jakšić et al., 2012) and later in renal ACHN cells, colorectal LS-174T cells and hepatic HepG2 cells (Theumer et al., 2018). The presence of VerA in foodstuffs therefore raises concerns about its toxicity for the digestive tract. As the intestinal barrier is the first line of defense encountered by contaminants after intake, the aim of the present study was to investigate the toxicity process induced by VerA in intestinal cells. Since the p53 tumor suppressor plays a key role in the control of apoptosis and cell cycle arrest (Pucci et al., 2000; Speidel, 2015; Vousden and Prives, 2009) we compared the toxic process of AFB_1 and VerA in intestinal cell lines with different p53 status: p53 wild-type expressing cells (p53 wt HCT116 cells), p53 suppressed cells (p53-/- HCT116 cells) and mutated p53 cells (Caco-2 cells).

2. Materials and methods

2.1. Mycotoxins

AFB_1 was purchased from Sigma-Aldrich (Saint Quentin Fallavier, France). VerA was obtained from *Aspergillus parasiticus* SRRC 0164 strain cultured on wheat grains. Briefly, after pre-culture in plates containing potato dextrose agar (PDA) at 28 °C for 7 days, small portions of this culture were transferred and dispersed in 14 cm diameter Petri dishes containing autoclaved wheat. Water activity of the grains was measured with an HC2-AW device (Rotronik AG, Basserdorf, Switzerland) and adjusted to 0.98 with sterile water. The inoculated plates were incubated at 28 °C for 7 days. At the end of the incubation period, wheat and mycelium were harvested and extracted overnight with chloroform. The chloroformic extract was filtered, clarified and evaporated to dryness as previously described (Theumer et al., 2018).

VerA was purified with an Ultimate 3000 HPLC system (Dionex/ThermoScientific, Courtaboeuf, France). A Strategy C18-2 semi-preparative column was used (length: 250 mm, internal diameter: 7.8 mm and particle size: 5 µm, Interchim, Montluçon, France). Purification was achieved by gradient elution using 0.1% acetic acid (eluent A) and acetonitrile (eluent B) as mobile phase at a flow rate of 4.2 mL/min. Elution started in 47% eluent B for 17 min. Then the proportion of eluent B was increased to 50% within 14 min, the column was rinsed with 90% eluent B for 4 min, and the elution gradient was reduced to the initial value over a period of 10 min and held constant for the last 15 min. The multiple fractions containing VerA were collected with an ultimate 3000 Fraction Collector (Dionex/ThermoScientific, Courtaboeuf, France) and pooled. The solvent was evaporated under reduced pressure with a Rotavapor® R-215 (Büchi, Flawil, Switzerland). Prior to toxicity experiments, the identity and purity of the purified VerA was confirmed by several methods described previously (Theumer et al., 2018).

Since fluorescence assays were used in the present study, it was checked that aqueous solutions of AFB_1 and VerA did not generate fluorescence using 400 to 500 nm excitation wavelengths.

2.2. Cell lines and growth conditions

Caco-2 cells were obtained from American Type Culture Collection (ATCC, Manassas, VA, USA). Isogenic p53 wild-type and p53 -/- HCT116 cell lines were kindly provided by Dr. Bert Vogelstein (Johns Hopkins University, Baltimore, MD, USA). The human colorectal adenocarcinoma cell line Caco-2 and the human colorectal carcinoma HCT116 cells were grown in Dulbecco's Modified Eagles Medium (DMEM) glutamax (Gibco, Saint-Aubin, France) supplemented with 0.5% gentamycin (10 mg/mL) and 10% fetal calf serum (FCS) from Eurobio (Les Ulis, France), and 1% MEM Non-essential Amino Acid Solution (Sigma-Aldrich, Saint Quentin Fallavier, France). To obtain differentiated Caco-2 cell layers mimicking intestinal epithelium, 60×10^3 cells were seeded in 0.3 cm^2 Transwell® inserts incorporating polyethylene terephthalate membrane with 3 µm pores (BD Biosciences, Franklin Lakes, NJ, USA). TEER (TransEpithelial Electrical Resistance) was recorded every two hours using a cellZscope device (NanoAnalytics GmbH, Munster, Germany). Cells were cultured for three weeks to obtain a 300 $\Omega \cdot cm^2$ electrical resistance indicating a confluent cell layer and then were exposed to toxins for 48 h.

2.3. Simultaneous quantification of VerA and AFB_1 in Caco-2 culture medium

AFB_1 and VerA concentrations were simultaneous assayed by High-Performance Liquid Chromatography (HPLC) coupled with Diode Array Detector (DAD) (Thermo Electron Corporation, Waltham, MA, USA). One hundred microliters of acetonitrile containing Internal Standard (sterigmatocystin 1 µg/mL) were added to 100 µL of cell culture medium samples. The mixture was briefly vortexed and centrifuged for 10 min at 20 000*g* at 4 °C. Supernatant was transferred into HPLC vials and 20 µL were injected into HPLC system. Chromatographic separation was achieved on a Phenomenex Luna C18 column (150 × 2 mm; 5 µm) at 20 °C. A gradient elution was performed at flow rate of 300 µL/min with H_2O acidified by 0.1% acetic acid (A) and acetonitrile (B) as mobile phase under the following conditions: elution started in 50% B and the proportion of eluent B was increased to 90% within 15 min; the column was rinsed with 90% B for 10 min; then the elution gradient was reduced to 50% B within 5 min; finally the column was re-equilibrated in 50% B for 10 min. The DAD wavelength was set at 288 nm for VerA, 362 nm for AFB_1 and 329 nm for sterigmatocystin. Chromatographic data were monitored by Chromeleon® software (Thermo Electron Corporation, Waltham, MA, USA). Calibration curve was used for quantification with a linear model weighted by $1/x^2$ (x = concentration) obtained from blank cell culture medium spiked with AFB_1 and VerA mixture at concentration ranging from 0.1 to 10 µg/mL.

2.4. Cytotoxicity assessment by CellTiter-Glo assay

The luminescent CellTiter-Glo assay (Promega, Madison, USA) previously described in Tannous et al., 2017 (Tannous et al., 2017) was used to measure ATP as an indicator of cell viability following 48 h exposure to increasing concentrations of VerA and AFB_1. Indeed, the level of ATP being proportional to the number of living cells and to the cell metabolic activity, it makes ATP a relevant endpoint to measure cytotoxicity. Caco-2 cells were exposed to VerA from 0.3 µM to 30 µM and to AFB_1 from 1.8 µM to 60 µM. HCT116 cells were exposed to VerA or AFB_1 from 0.5 µM to 50 µM. The luminescence was recorded using the Infinite 200 Pro multimode microplate reader (Tecan, Lyon, France). IC_{50} value was defined as the concentration that induced a 50% decrease in measured ATP compared to the control.

2.5. Detection of apoptotic cells

The apoptotic process involves different steps from its initial induction to the final cell death. We focused on three important steps: activation of caspase 3/7 activation, phosphatidylserine exposure to the outer membrane leaflet and fragmentation and condensation of the nuclear chromatin. Detecting early and late events of the apoptotic process makes the results more reliable.

2.6. Caspases 3/7 activity

Activation of caspases 3/7 is a key event in the apoptotic process. Active caspases were detected by flow cytometry using CellEvent™ Caspase3/7 Green Detection Reagent (Molecular Probes, Madison, WI, USA). Apoptosis was assessed after 48 h of exposure to either VerA or AFB_1. In practice, 100 × 10^3 HCT116 cells were seeded in 24 well plates (Greiner Bio-One, Les Ulis, France) and cultured for one day in DMEM supplemented with 10% FCS. The medium was then removed and the cells were exposed for 48 h to 10% FCS medium containing either VerA or AFB_1 at 10 and 20 μM. The culture medium was collected and cells were harvested using Gibco® 0.05% trypsin - EDTA (Life Technologies, Paisley, UK). After centrifugation at 450*g* for 10 min, the supernatant was discarded, and the cells were suspended in 1 mL 10% FCS - DMEM medium containing 2 μM CellEvent™ Caspase3/7 Green and incubated for 30 min at room temperature. After staining, the cells were centrifuged at 450*g* for 6 min and suspended in 300 μL Running Buffer (Miltenyi Biotec, Bergisch Gladbach, Germany). To identify necrotic cells, 0.2 μM Topro-3 (Molecular Probes, Madison, WI, USA) was added just before analysis.

2.7. Phosphatidylserine (PS) translocation

PS exposure to the outer leaflet of the plasma membrane is a hallmark of apoptotic cells. These cells were detected using the Pacific Blue™ Annexin V/Dead Cell Apoptosis assay (Molecular Probes, Madison, WI, USA). First, 100 × 10^3 HCT116 cells or 50 × 10^3 Caco-2 cells were seeded in 24-well plates (Greiner Bio-One, Les Ulis, France) and cultured for one day in DMEM supplemented with 10% FCS. The medium was then removed and the cells were exposed for 48 h to fresh medium containing either VerA or AFB_1 at 0.25 to 20 μM. The cells were stained according to the manufacturer's instructions. To identify necrotic cells, 0.2 μg propidium iodide (Molecular Probes, Madison, WI, USA) was added just before analysis.

Fluorescence was measured using a MACSQuant™ Analyser 10 cytometer (Miltenyi Biotec GmbH, Bergisch Gladbach, Germany). The data were calculated using Venturi software (Applied Cytometry, Sheffield, UK).

2.8. Assessment of apoptotic nuclei

Nuclear chromatin staining enables the identification of fragmented and condensed nuclei, a hallmark of apoptosis. After 48 h exposure to mycotoxins, cellular nuclei were stained using 5 μg/mL Hoechst 33,342 (Molecular Probes, Madison, WI, USA) at 37 °C for 20 min. Images were recorded with an EVOS™ inverted microscope (Ozyme, Saint-Quentin Yvelines, France).

2.9. Real-time proliferation

Caco-2 cells (6 × 10^3) or HCT116 (4 × 10^4) cells were seeded in each well of an E-Plate 16 PET chamber and the electrical impedance signal (CI) was recorded in an xCELLigence real-time analyzer (ACEA Biosciences Inc., San Diego, CA, USA). Cells were cultured for 24 h before mycotoxins were added. A growth coefficient ratio was calculated for each mycotoxin after 48 h exposure (72 h of culture): $(CI_{72hr} - CI_{24hr})_{mycotoxins}$ / $(CI_{72hr} - CI_{24hr})_{control}$.

2.10. Cell cycle analysis

HCT116 cells (100 × 10^3) or Caco-2 cells (50 × 10^3) were seeded in 24-well plates (Greiner Bio-One, Les Ulis, France) and treated with AFB_1 or VerA for 48 h. The cell cycle was investigated using the Click-iT EdU Alexa Fluor® 647 Flow Cytometry Assay kit (Sigma-Aldrich, Saint-Louis, MO, USA) according to the manufacturer's instructions. The cells were then washed and suspended in 0.5 mL of PBS containing 4 μM 4′6′-diamidino-2-phenylindole (DAPI) at room temperature for 20 min. Fluorescence was recorded using a flow cytometer (MACSQuant Analyzer 10, Miltenyi Biotec, Bergisch Gladbach, Germany). The data were calculated using Venturi software (Applied Cytometry, Sheffield, UK).

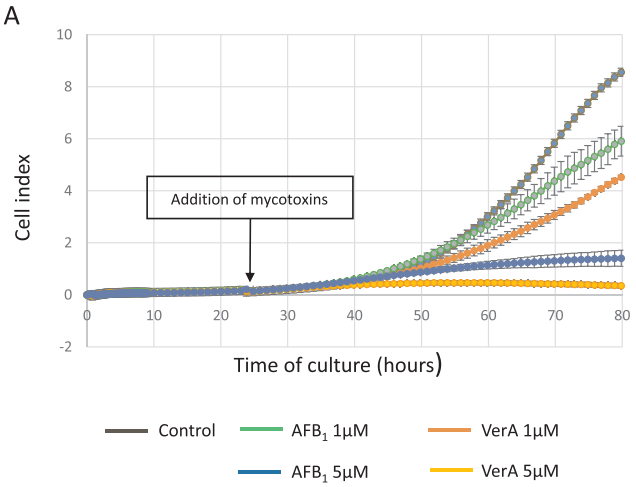

Fig. 1a. Toxicity of VerA and AFB_1 for Caco-2 cells. Effect on cell proliferation over a period of 48 h: cells were seeded in a 16-well chamber placed in the real-time analyzer xCELLigence. Cell indexes (CI) were recorded over a period of 72 h. Mycotoxins were added 24 h after seeding cells and the vehicle DMSO (control) was added to the untreated cells.

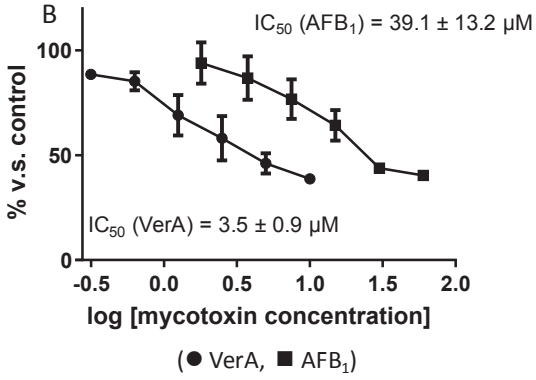

Fig. 1b. Dose response toxicity after 48 h of exposure to mycotoxins (● VerA; ■AFB_1): cells were seeded in 96-well plates and cultured for 24 h before addition of mycotoxins (from 0.3 to 10 μM VerA or 1.8 to 60 μM AFB_1). ATP content was measured after 48 h of exposure to mycotoxins using the CellTiter Glo assay. Values are expressed as a percentage of the results obtained with the untreated control cells.

2.11. Western blot analysis of phospho-p53

HCT116 cells were cultured in Petri dishes for 24 h (5 × 10^6 cells/well in 10 mL of DMEM) before being treated with 10 μM and 20 μM AFB_1 or VerA for 48 h. Cell layers were then washed with ice-cold PBS and then lysed at 4 °C for 30 min in 300 μL RIPA buffer containing anti-protease (0.1% SDS, 1% Triton X-100, 0.5% sodium deoxycholate, 150 mM NaCl, 50 mM TRIS pH 8.0, 1.0 mM sodium *ortho*-vanadate, 1 mM PMSF, 5 mM EDTA). After centrifugation at 13 500*g* at 4 °C for 20 min, the supernatant was boiled at 100 °C for 5 min in a Laemmli buffer (2% SDS, 50 mM DTT, 10% glycerol, 62 mM TRIS pH 6.8). Electrophoresis was run on 4–20% SDS-PAGE and proteins were transferred to PVDF membrane. The membranes were saturated for 2 h with a 1/1 mixture of blocking buffer (Rockland, Immunochemicals Inc., Limerick, PA, USA) and Tris Buffer (150 mM NaCl, 20 mM TRIS,

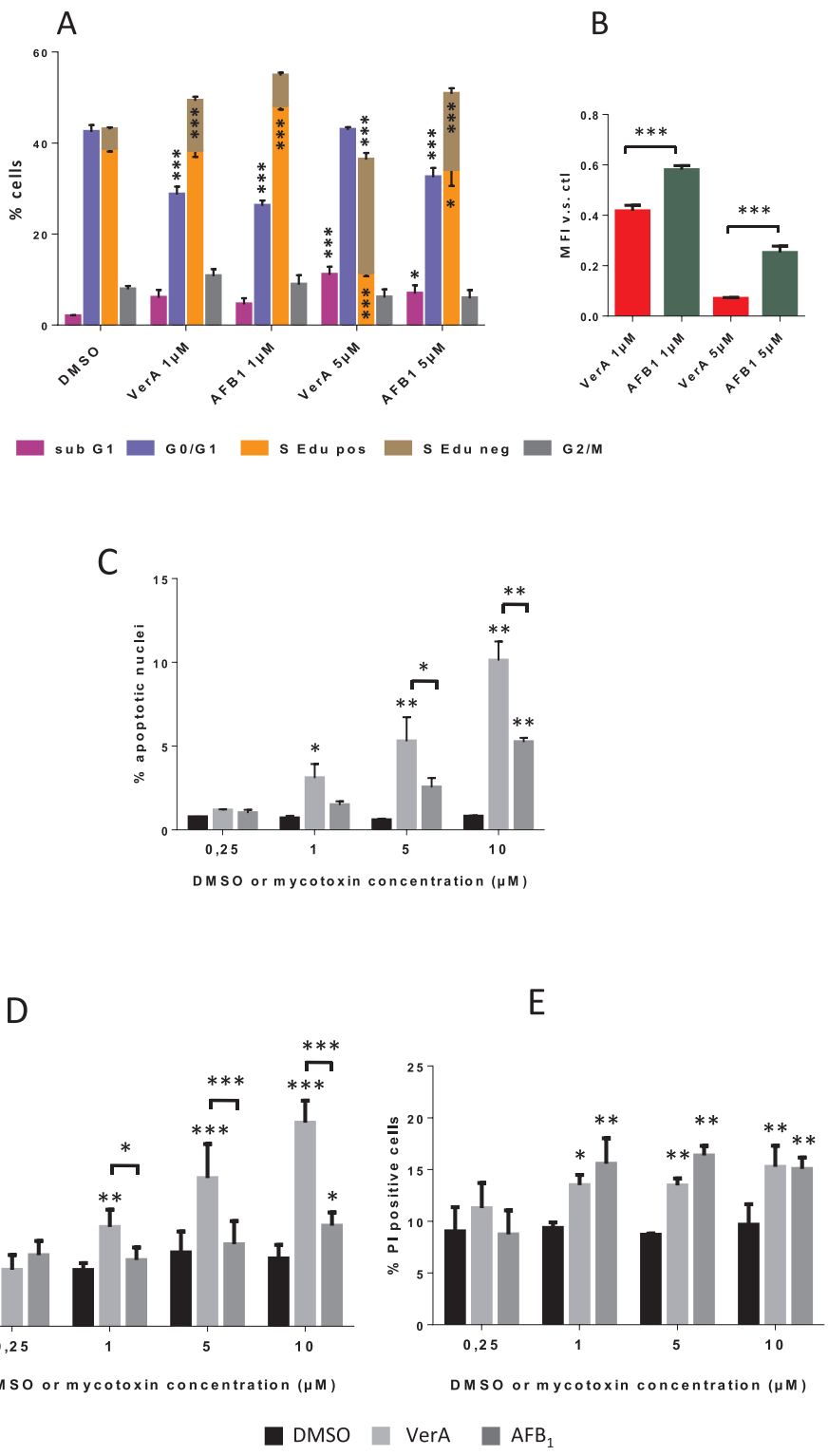

Fig. 2. Effect on the cell cycle and induction of apoptosis in Caco-2 cells. Cells were exposed to VerA, AFB_1 or DMSO for 48 h at the concentrations indicated. **(A)** Double staining with DAPI and Edu-Alexa Fluor® 647 revealed the DNA content and S-phase cells displaying DNA synthesis, respectively. Cell cycle phases were analyzed by flow cytometry. S-phase cells were divided into replicative (S Edu pos.) and non-replicative cells (S Edu neg.). **(B)** Alexa Fluor® 647 mean fluorescence intensity (MFI) of S-phase replicative cells were normalized as fraction relative to DMSO. **(C)** Nuclei were stained with Hoechst 33342. Normal and condensed/fragmented nuclei were counted under a fluorescent microscope and the percentage of apoptotic nuclei was calculated. **(D)** and **(E)** Cells stained with annexin-V- Pacific Blue™ and propidium iodide (PI). Cell populations were analyzed by flow cytometry. **(D)** Percentage of apoptotic annexin-V positive cells (negative for PI). **(E)** Percentage of permeabilized (necrosis or late apoptosis) cells. Values are means and errors bars indicate SEM from three independent experiments (* $p < 0.05$; ** $p < 0.01$; ***$p < 0.001$ according to ANOVA).

pH 7.5) and incubated at 4 °C overnight with either a rabbit anti-human phospho (Ser15) - p53 (Cell Signaling Technology, Danvers, MA, USA), or a rabbit anti-human β-actin antibodies (Cell Signaling Technology, Danvers, MA, USA), diluted 1:500 in TBS blocking buffer. After washing, the membranes were incubated with 1:10000 CF™770 conjugated anti-rabbit IgG (Biotium Inc., Fremont, CA, USA) at room temperature for one hour. Membranes were analyzed using an Odyssey Infrared Imaging System (LI-COR, ScienceTec, Les Ulis, France). Fluorescence intensities were determined using LI-COR imaging software after correction for background signal. The expression of the proteins was estimated after normalization calculated with the ratio of the intensity of the band of interest and of the actin band as already described (Pinton et al., 2012).

2.12. Western blot analysis of checkpoint kinase 1, phospho-Checkpoint kinase 1, checkpoint kinase 2 and phospho-Checkpoint kinase 2

Cells were incubated on ice for 30 min in lysis buffer (50 mM Tris-

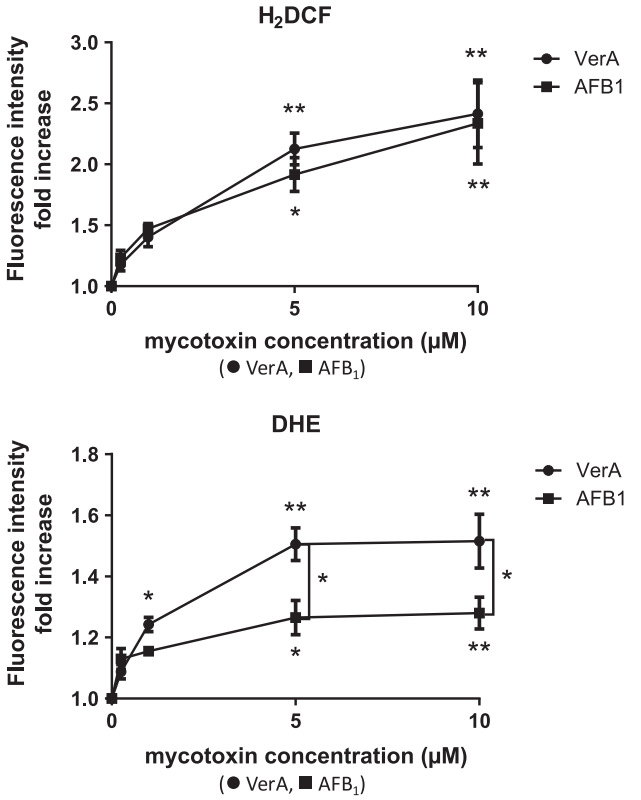

Fig. 3. Detection of reactive oxygen species (ROS). Caco-2 cells were treated with increasing concentrations of VerA and AFB_1 for 48 h. H_2DCF-DA and DHE were used to detect hydrogen peroxide and superoxide anion, respectively. Cells were analyzed by flow cytometry. A fold increase in ROS content corresponds to the value resulting from the ratio of the mean fluorescence intensity (MFI) obtained with treated and control cells. All values are means and errors bars indicate SEM from five and four independent experiments for H2DCF and DHE respectively (* $p < 0.01$; ** $p < 0.001$ according to ANOVA).

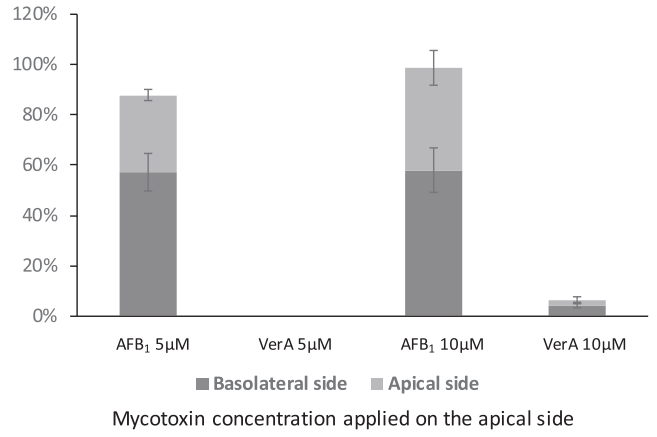

Fig. 4. Caco-2 cell monolayers cultured on inserts were exposed for 48 h to 5 and 10 μM of VerA or AFB_1 applied on the apical side. Mycotoxins from the basolateral and apical sides were analyzed by HPLC before and after treatment. Data represent the rate of mycotoxins recovered in each compartment compared to the initial quantity. Values are means and errors bars indicate the SEM of the data (n = 3).

HCl pH 7.5, 250 mM NaCl and 0.5% NP40) containing the Halt™ Protease & Phosphatase inhibitor cocktail (Thermo Scientific, Rockford, IL, USA) and sonicated. Cell lysates were centrifuged and the supernatant containing total soluble proteins was kept. Proteins were separated by SDS-PAGE and transferred to an Amersham nitrocellulose membrane (GE Healthcare, Pittsburgh, PA, USA). Membranes were incubated with the primary antibody for 1–16 h. Chk1 (2G1D5), pChk1 (133D3), Chk2 (1C12) and pChk2 (C13C1) antibodies (dilution 1:1000) were purchased from Cell Signalling Technology, Inc., (Danvers, MA, USA). GAPDH antibody (GTX100118, dilution 1:10 000) was purchased from Genetex (Genetex Developments Ltd, London, UK). The secondary anti-mouse or anti-rabbit HRP-conjugated antibodies (Jackson Immunoresearch laboratories, Baltimore, PE, USA) were incubated at room temperature for 1 h. Proteins were revealed with the enhanced chemiluminescence substrate ECL (Bio-Rad, Hercules, CA, USA) and imaged using the ChemiDoc XRS Biorad Imager and Image Lab Software (Bio-Rad, Hercules, CA, USA).

2.13. Detection of reactive oxygen species (ROS)

Caco-2 cells were treated with increasing concentrations of VerA and AFB_1 for 48 h and ROS were detected as previously described (Gauthier et al., 2012). Cells were harvested by trypsination and centrifugation and then suspended in HBSS buffer containing 5 μM dihydroethidium (DHE, Molecular Probes, Madison, WI, USA) to detect superoxide anion or 10 μM dichlorodihydrofluorescein diacetate (H_2DCF-DA, Molecular Probes, Madison, WI. USA) to detect hydrogen peroxide. Menadione (100 μM) was used as positive control (Sigma-Aldrich, St. Louis, MO. USA). Cells were incubated at 37 °C in the dark for 20 min. After washing the cells with 2 mL HBSS (Hank's Balanced Salt Solution) buffer, cells were suspended in 0.5 mL HBSS buffer for cytometry analysis (Miltenyi Biotec GmbH, Bergisch Gladbach, Germany). Dead cells were stained by adding 0.2 μM Topro-3 (Molecular Probes, Madison, WI. USA). The data were calculated using Venturi software (Applied Cytometry, Sheffield, UK).

2.14. DNA strand break analysis and DAPI staining for micronucleus and mitotic index quantification

Caco-2 cells were grown on glass coverslips. After at least 24 h of culture, the cells were fixed with 4% paraformaldehyde, washed in PBS and stained with DAPI for micronucleus and mitotic index quantification. For immunofluorescence analyses, fixed cells were permeabilized with 0.5% Triton X-100 for 15 min, blocked in 3% BSA and stained with primary antibodies (dilution 1:1000) in blocking solution for 2 h. 53BP1 (NB100-304) antibody was purchased from Novus Biologicals (Centennial, CO, USA) and γH2AX antibody (05–636) from Merck/Millipore (Darmstadt, Germany). Cells were washed three times with PBS-Tween 0.1% and incubated with secondary antibodies (dilution 1:800) for 1 h (Rhodamine Red X (R6394) and Alexa Fluor 488 Goat anti-mouse (A11017) or anti-rabbit (A11070), purchased from Invitrogen (Carlsbad, CA, USA). DNA was stained with DAPI. Images were acquired using a fluorescent Nikon Eclipse 50i microscope equipped with a 20x objective and then processed with ImageJ software. The average gray value of each nucleus was measured for at least 500 nuclei. Values were compiled on a scatter plot and mean fluorescence intensity was calculated for each treatment.

2.15. Comet assay

To induce DNA damage as products of purine oxidation detectable by formamidopyrimidine-DNA glycosylase (Fpg), the cells were placed on ice and treated with 1 μM Ro 19-8022 (a gift from Hoffman Laroche Ltd, Switzerland) for 2 min 30 sec under visible light (1000 W-halogen). Ro 19-8022 plus light is an appropriate positive control for the Fpg-modified comet assay (Azqueta et al., 2013). Trypsinized Caco-2 cells were embedded in 0.7% low melting point agarose (Sigma-Aldrich, Saint-Louis, MO, USA) and in parallel digestion with Fpg enzyme (gift from Serge Boiteux, CNRS, France) allowing the detection of Fpg-sensitive sites, as previously described (Azqueta et al., 2013). A comet assay was performed as previously described (Perdry et al., 2018). Fifty

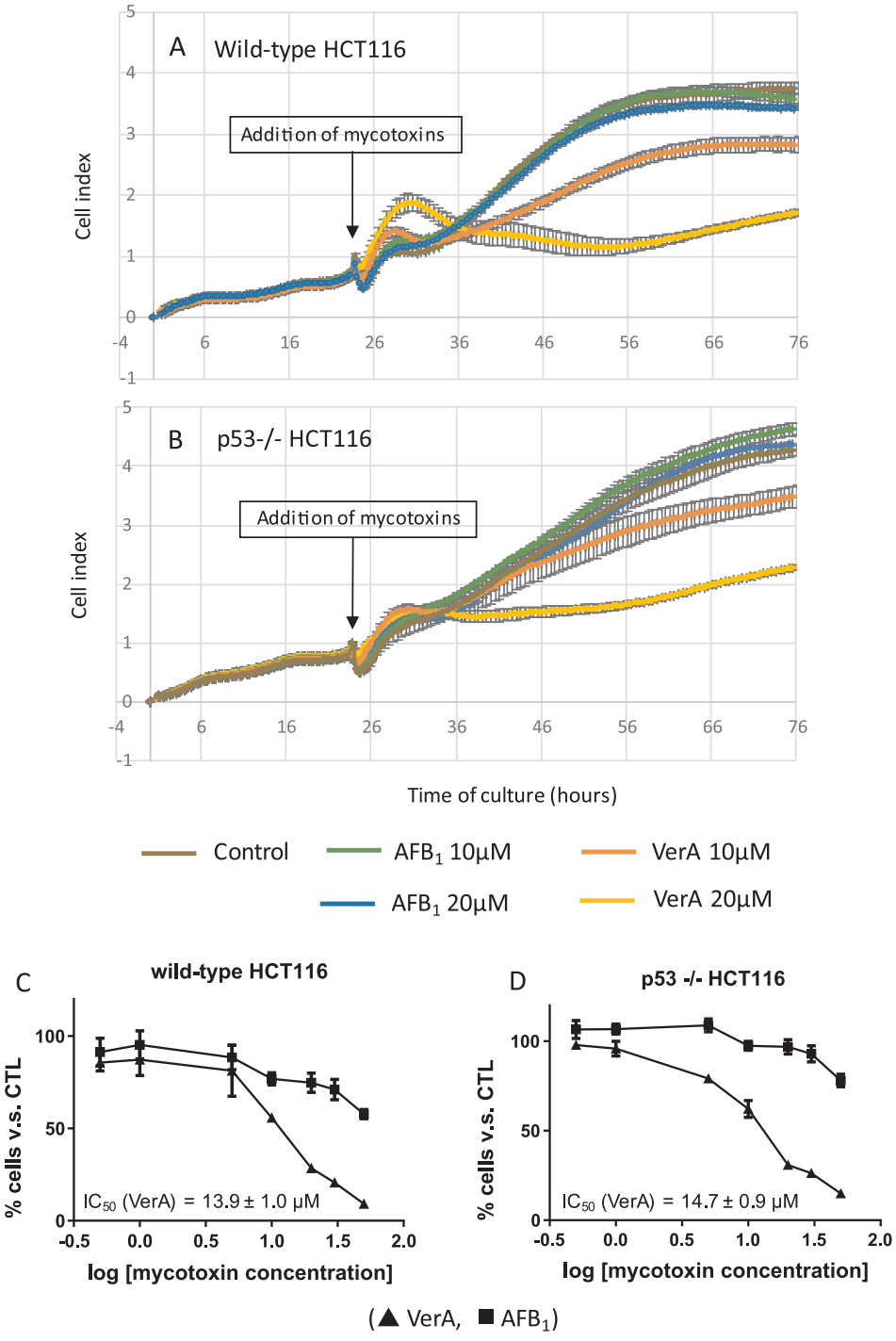

Fig. 5. Toxicity of VerA and AFB_1 for HCT116 cells. (**A**) Effect on cell proliferation over a period of 48 h: cells were seeded in a 16-well chamber placed in the real-time analyzer. Cell indexes (CI) were recorded over a period of 72 h. Mycotoxins were added 24 h after seeding cells and the vehicle DMSO was added to the untreated cells. (**C**) and (**D**) Dose response toxicity after 48 h of exposure to mycotoxins (▲VerA; ■AFB_1): cells were seeded in 96-well plates and cultured for 24 h before from 0.5 to 50 µM mycotoxins were added. ATP content was measured after 48 h of exposure to the mycotoxins. Values are expressed as a percentage of the results obtained with the untreated control cells.

cells per deposit and two deposits per sample were analyzed. The extent of DNA damage was evaluated for each cell by measuring the intensity of all tail pixels divided by the total intensity of all pixels in the head and tail of the comet. The median of these 100 values was calculated and named % tail DNA. Fpg-sensitive sites (% Tail DNA) were obtained for each condition by subtracting the damage (% Tail DNA) obtained in the absence of Fpg from Fpg-exposed comets ("+Fpg" − "-Fpg" = Fpg sensitive sites).

2.16. Microarray analysis

In order to evaluate the impact of VerA and AFB_1 on the global transcriptome, 1.5×10^5 Caco-2 cells were seeded in six-well flat bottom plates and inoculated at 37 °C for 24 h. After incubation, the cells were treated with 1 µM VerA, 1 µM AFB_1 and DMSO for the control. After 24 h of incubation, mRNAs were extracted and processed for labeling and hybridized for Agilent SurePrint G3 Human GE 8x60K microarray (Agilent technology, Santa Clara, USA) as previously described (Tannous et al., 2017). All data and experimental details are available in the Gene Expression Omnibus (GEO) database under accession number GSE75934. Microarray data were analyzed with R software (R Core Team., 2018), using the Bioconductor packages (Huber et al., 2015). The limma package (Ritchie et al., 2015) was used to analyze differences between treatments. A model was fitted using the limma lmFit function (Smyth, 2004). A correction for multiple testing was then applied using the False Discovery Rate (Benjamini and

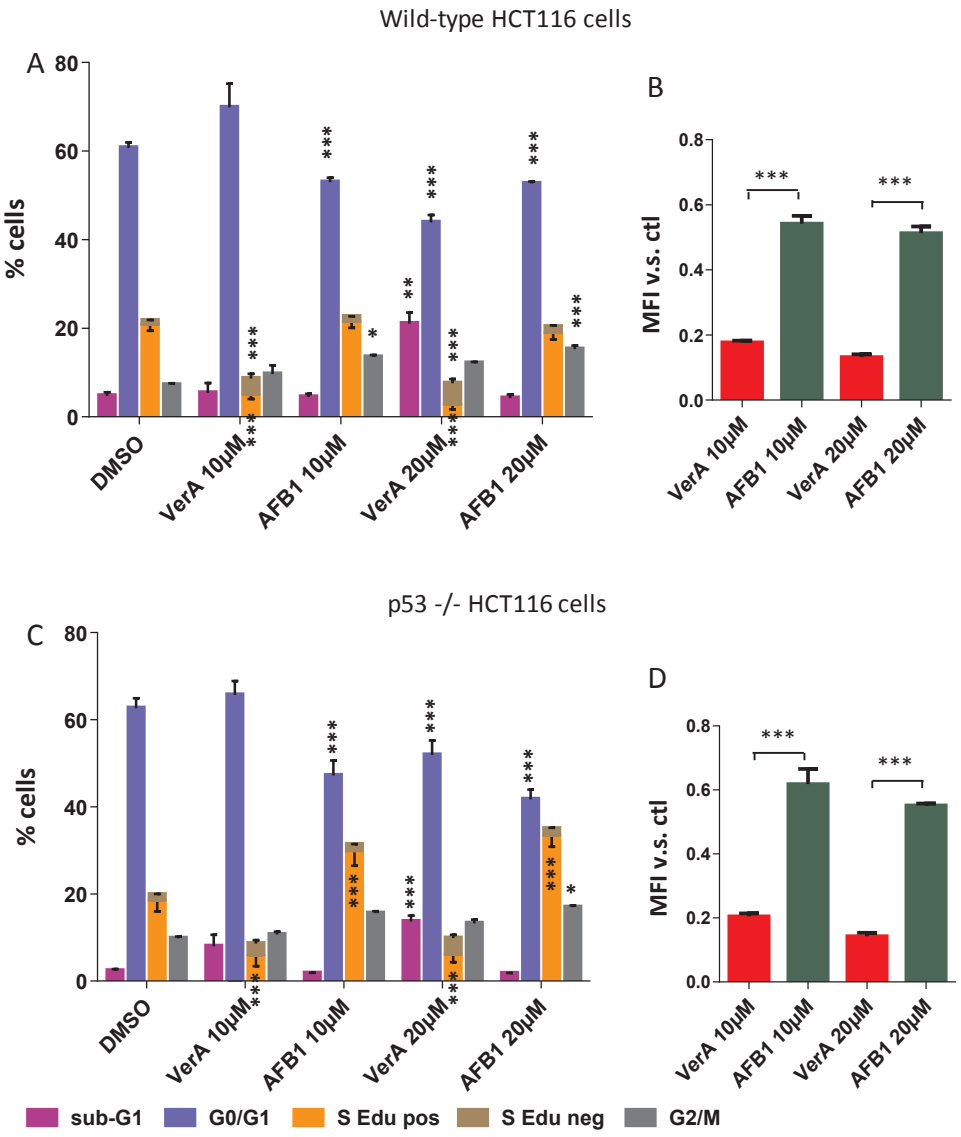

Fig. 6. Impact of HCT116 cells on the cell cycle. Wild Type and p53-/- HCT116 cells were exposed to VerA and AFB_1 for a period of 48 h at the concentrations indicated. **(A)** and **(C)** Double staining with DAPI and Edu-Alexa Fluor® 647 revealed the DNA content and S-phase cells displaying DNA synthesis, respectively. Cell cycle phases were analyzed by flow cytometry. S-phase cells were divided into replicative (S Edu pos.) and non-replicative cells (S Edu neg.). **(B)** and **(D)** Alexa Fluor® 647 mean fluorescence intensity (MFI) of S-phase replicative cells were normalized as fractions relative to DMSO. Values are means and errors bars indicate SEM from three independent experiments (* $p < 0.05$; ***$p < 0.001$ according to ANOVA).

Hochberg, 1995). Probes with FDR ≤ 5% were considered differentially expressed in treated and control conditions. Hierarchical clustering was applied to the samples and the probes using the 1-Pearson correlation coefficient as distance and the Ward's criterion for agglomeration.

2.17. Statistical analysis

The results were analyzed using GraphPad Prism™ version 6 software (GraphPad Software, La Jolla, CA, USA). One-way ANOVA was used to analyze the difference between the mycotoxin treatments within a cell population and two-way ANOVA to compare results between groups.

3. Results

3.1. Cytotoxic potency of VerA and AFB_1 for Caco-2 cells

We first determined the capability of AFB_1 and its precursor VerA to inhibit the growth rate of Caco-2 cells. After addition of mycotoxins, real-time proliferation was recorded for 48 h using the xCELLigence device (Fig. 1a) and a proliferation coefficient was calculated after 48 h of exposure to the mycotoxins (Table S1). At 1 µM, VerA was more potent in slowing down Caco-2 cell proliferation than AFB_1 whereas 5 µM of both mycotoxins severely inhibited cell growth.

A dose-respond study was performed during the 48-hour period of exposure using the CellTiter Glo assay (Fig. 1b). IC_{50} values were calculated from the dose-response curves obtained for each cell type (Table S2). VerA had higher cytotoxic potency than AFB_1 as shown by the tenfold lower IC_{50} value obtained for VerA compared to AFB_1.

The effect of the two toxins on the cell cycle was investigated to check if the slowdown in cell proliferation was related to a perturbation of the cell division machinery. The cell cycle was analyzed after 48 h of exposure to mycotoxins. In Caco-2 cells, VerA decreased or even stopped the DNA replication of S-phase cells in a dose dependent manner (Fig. 2A–B) leading to the accumulation of S-phase cells at 1 µM VerA and appearance of apoptotic sub-G1 particles at 5 µM VerA. AFB_1 produced the same effect as VerA but to a lesser extent. To elucidate whether an apoptotic process was involved in the cytotoxicity induced by VerA and AFB_1 we assessed the induction of apoptosis after 48 h of exposure to the two mycotoxins. Counting of fragmented and condensed nuclei and AnnexinV/PI staining enable to detect apoptotic cells at two different stages of the cell death process. Both methods showed that VerA triggered apoptosis in Caco-2 cells from 1 µM while a lower but significant increase in apoptotic hallmarks was detected only in cells treated with 10 µM AFB_1 (Fig. 2C–D). Both mycotoxins induced a

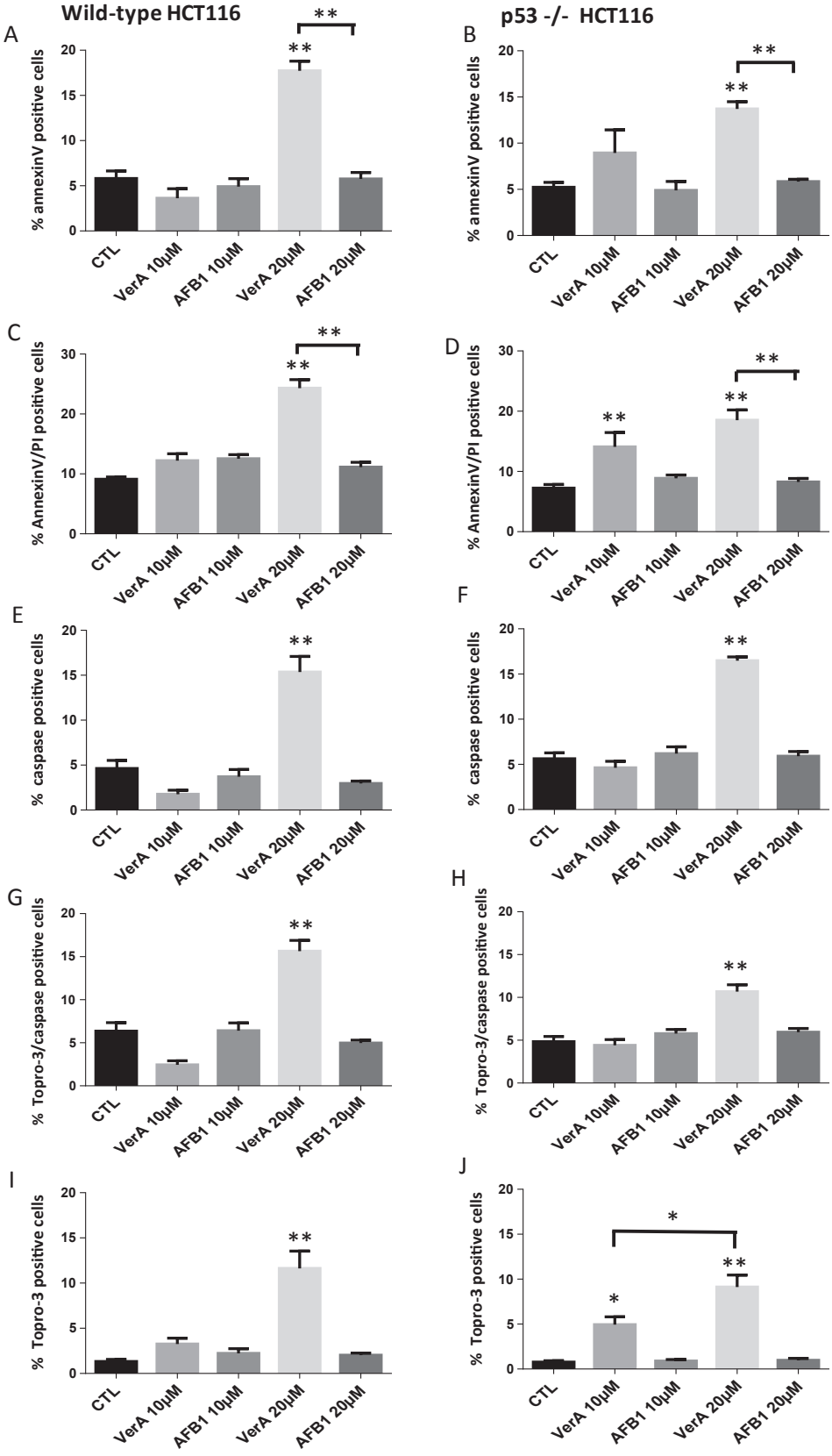

Fig. 7. Induction of apoptosis in HCT116 cells. Cells were exposed to 10 µM and 20 µM of VerA and AFB_1 for 48 h. **(A), (B), (C), (D)** Cells were stained with annexin-V/Pacific Blue™ and propidium iodide (PI). (A), (B) Percentage of apoptotic annexin-V positive cells. (C), (D) Percentage of permeabilized (necrosis or late apoptosis) PI positive cells. **(E), (F), (G), (H), I), (J)** Cells were stained with CellEvent Green™ and Topro-3. (E), (F) Cells displaying caspase 3/7 activity. (G), (H) Permeabilized cells displaying caspase 3/7 activity. (I), (J) Permeabilized dead cells. Cell populations were analyzed by flow cytometry. Values are means and errors bars indicate SEM from four independent experiments (* $p < 0.05$; ** $p < 0.001$ according to ANOVA).

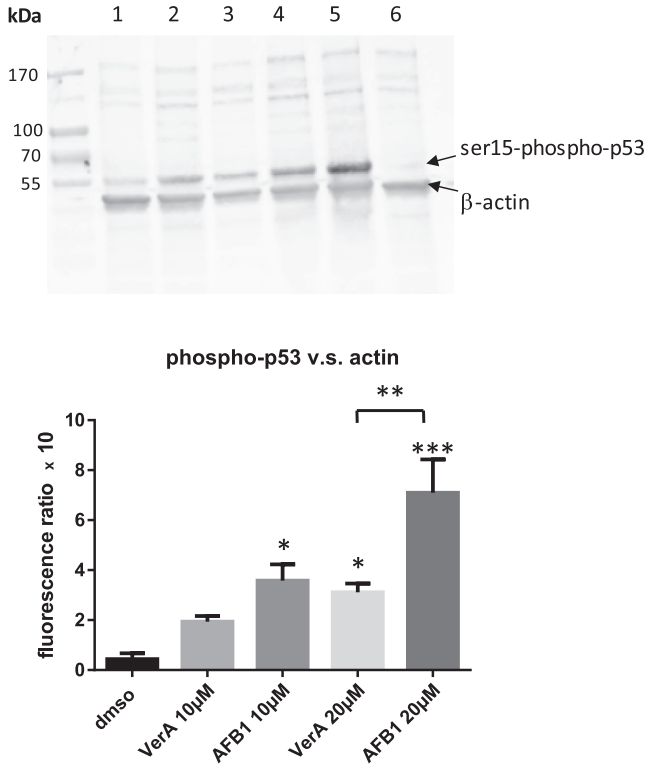

Fig. 8. VerA and AFB_1 induce p53 phosphorylation in a dose dependent manner. Wild-type HCT116 were cultured for 48 h in the presence of 10 μM and 20 μM VerA or AFB_1 before phosphorylated-p53 was detected by SDS/PAGE and Western blot analysis. **(A)** line 1: VerA 10 μM; line 2: AFB_1 10 μM; line 3: VerA 20 μM; line 4: AFB_1 20 μM; line 5: etoposide 50 μM; line 6: DMSO. **(B)** Values represent ratio versus β-actin. Values are means and errors bars indicate SEM from three independent experiments (* $p < 0.05$; ** $p < 0.01$; *** $p < 0.002$ according to ANOVA).

steady state level of permeabilized propidium iodide (PI) positive cells (Fig. 2E), which could be the signature of cell necrosis or late apoptosis.

3.2. Production of ROS after VerA and AFB_1 exposure

Reactive oxygen species (ROS) play important roles in cell death and signaling (Thannickal and Fanburg, 2000). Indeed, ROS can induce intrinsic apoptosis by triggering DNA damage and conversely, DNA damage can stimulate the production of ROS (Kim et al., 2012; Zhang et al., 2015). Since it has already been demonstrated that AFB_1 can concomitantly induce oxidative stress and apoptosis in broiler hepatocytes (Liu and Wang, 2016), chicken thymocytes (Peng et al., 2016), bursa of Fabricius cells (Yuan et al., 2016) and HepG2 cells (Yang et al., 2016), we sought to determine whether VerA and AFB_1 could trigger ROS production in Caco-2 cells. Our results (Fig. 3) showed that exposure to both mycotoxins increased ROS content and that treatment with VerA was able to generate more superoxide anion than AFB_1.

3.3. Transfer of VerA and AFB_1 from the apical to the basolateral side of the epithelial cell layer

When cultured on inserts for three weeks, Caco-2 cells differentiate to form a polarized epithelial cell monolayer that provides a physical and biochemical barrier to additives. When 5 or 10 μM VerA or AFB_1 was added to the apical upper side of the inserts for 48 h, they did not have the same fate. Whereas 57% of AFB_1 was recovered in the basolateral down side, no or almost no VerA was detected either from the apical side or from the basolateral side, suggesting its sequestration and/or biotransformation inside the cells (Fig. 4). Conversely, all the AFB_1 was distributed between the apical and basolateral sides.

3.4. Role of the p53 pathway in the cytotoxic process

Since Caco-2 cells do not harbor a functional p53 (Liu and Bodmer, 2006), we decided to investigate the influence of this protein on the cytotoxic potency of VerA and AFB_1 using deficient p53 -/- HCT116 cell lines and wild-type p53 HCT116 cells.

Proliferation of both HCT116 cell lines was less sensitive to both mycotoxins than Caco-2 cells. Indeed, HCT116 cells were not affected until 20 μM AFB_1 while their growth rate slowed down in the presence of 10 μM and 20 μM VerA in a dose dependent manner (Fig. 5A–B). Interestingly, 20 μM VerA inhibited the proliferation of wild-type HCT116 cells more severely than the proliferation of p53-/- HCT116 cells (Table S1). CellTiter Glo analysis confirmed that both HCT116 cells lines were less sensitive to VerA or AFB_1 than Caco-2 cells (Fig. 5C-D). However, no significant difference was observed when we compared the results obtained with wild-type and p53-/- HCT116 cells. Indeed, while AFB_1 had so few cytotoxic effects on the two HCT116 cell lines that IC_{50} could not be calculated, IC_{50} for VerA reached around 14 μM in both cases (Table S2).

In both wild-type and p53-/- HCT116 cells, exposure to 10 μM VerA reduced the S-phase cells and reduced their DNA replication (Fig. 6A-B-C-D). Furthermore, at 20 μM VerA, the resulting increase in sub-G1 particles indicated the induction of apoptosis. Unlike VerA, AFB_1 did not have the same effect in wild-type and p53-/- HCT116 cells: in wild-type HCT116 cells, AFB_1 triggered accumulation in the population in the G2/M-phase (Fig. 6A) whereas in p53-/- HCT116 cells it induced an accumulation in the population in S-phase (Fig. 6C). In both cases, the increase in dividing populations was accompanied by a decrease in the G1 population. Like VerA, exposure to AFB_1 led to a decline in DNA replication in S-phase cells, but to a lesser extent than after exposure to VerA (Fig. 6B and 6D). Treatment with AFB_1 did not induce sub-G1 particles, indicating the absence of apoptotic processes. It should be noted that despite this effect on the cell division, no obvious impact on HCT116 cell proliferation was observed.

In HCT116 cell lines, AnnexinV/PI (Fig. 7A-B-C-D) and CellEvent™ Green/Topro-3 (Fig. 7E-F-G-H) assays showed that neither VerA nor AFB_1 induced apoptosis up to a dose of 10 μM. However, in contrast to AFB_1, 20 μM VerA induced early (AnnexinV or activated caspase cells) and late (Topro-3/activated caspase cells) apoptosis in both wild-type and p53-/- HCT116 cells. The identification of Topro-3 only stained cells (Fig. 7I–J) evidenced the presence of necrotic dead cells after exposure to VerA but not to AFB_1.

Finally we explored the capacity of VerA to activate the p53 pathway. SDS/PAGE and Western blot analysis (Fig. 8) showed that exposure of wild-type HCT116 cells to 20 μM VerA led to a significant increase in phosphorylated p53, arguing for the involvement of the p53 pathway in the apoptotic process in HCT116 cells. However, an even greater increase in phosphorylated p53 was obtained when the cells were treated with AFB_1, without inducing apoptosis, supporting the hypothesis that the apoptotic process in HCT116 cells do not entirely rely on the p53 pathway.

3.5. Genotoxic potency of VerA and AFB_1 for Caco-2 cells

Given that AFB_1 is known to induce genotoxicity, we sought to compare the genotoxic potency of VerA and AFB_1 in Caco-2 cells. Considering that response to DNA damage involves serine 139 phosphorylation of the histone variant H2AX (Cook et al., 2009; Podhorecka et al., 2010) we first wanted to detect phosphorylated H2AX (γH2AX) after exposure to the mycotoxins. Caco-2 cells exposed to AFB_1 or VerA for 8 or 16 h exhibited a higher γH2AX staining than control cells (Figs. 9A and S2). Moreover, quantification of γH2AX signal showed that VerA induced more H2AX phosphorylation than AFB_1 at all the times and concentrations tested. This result suggests that VerA exposure

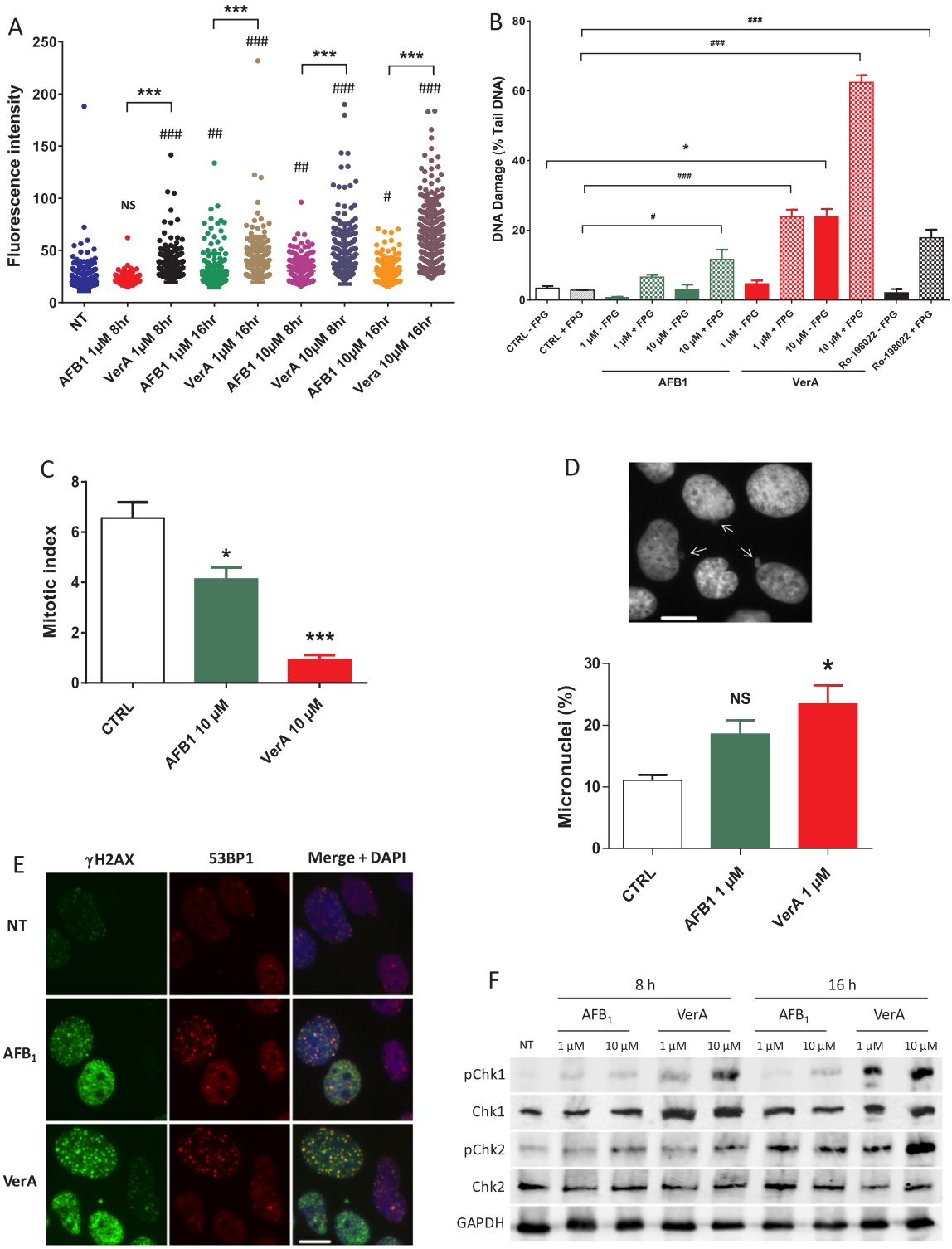

Fig. 9. Genotoxicity of VerA and AFB_1 to Caco-2 cells. **(A)** Quantification of γH2AX immunostaining after 1 µM or 10 µM of VerA and AFB_1 treatment for 8 and 16 h. The average gray value within each nucleus were measured using Image J software. Data were compiled on at least 500 nuclei and mean values were calculated for each experiment. Results of three independent experiments. ($^{\#}P = 0.005$; $^{\#\#}P < 0.0005$; $^{\#\#\#}P < 0.0001$ versus not treated, group; ***P < 0.0001 VerA versus AFB_1 group, ANOVA followed by Turkey's post-hoc test). **(B)** DNA damage evaluated by alkaline (-FPG) and Fpg-modified comet assay (+FPG) after treatment with 1 µM or 10 µM of VerA and AFB_1 for 16 h (or 2 min 30 sec treatment with Ro 19-8022, positive control of induction of FPG sensitive sites). Results are mean ± SEM of three independent experiments. (*P < 0.05 versus CTRL –FPG group; $^{\#}P < 0.05$ and $^{\#\#\#}P < 0.001$ versus CTRL + FPG group, ANOVA followed by Dunnett's post-hoc test). **(C)** Mitotic index after 16 h of treatment with 1 µM or 10 µM of VerA and AFB_1. Values correspond to the ratio of cells undergoing mitosis. Results are mean ± SEM of four independent experiments (*P < 0.05, ***P < 0.001 versus CTRL group, ANOVA followed by Dunnett's post-hoc test). **(D)** Micronucleus induction frequency after 1 µM of VerA and AFB_1 treatment for 16 h. Representative image of cells (upper panel) with micronuclei (white arrows) quantified by fluorescence visualization after DAPI staining. Micronucleus quantification (lower panel), data are expressed as the mean ± SEM of three independent experiments. (*P < 0.05 versus CTRL, ANOVA followed by Dunnett's post-hoc test). **(E)** Representative images of γH2AX and 53BP1 immunostaining of cells treated with 10 µM of VerA and AFB_1 for 8 h. Scale bar = 20 µm. **(F)** p-Chk1, Chk1, p-Chk2, Chk2, GAPDH immunoblots of soluble extracts from cells treated with VerA and AFB_1 for 8 or 16 h. NT means not treated.

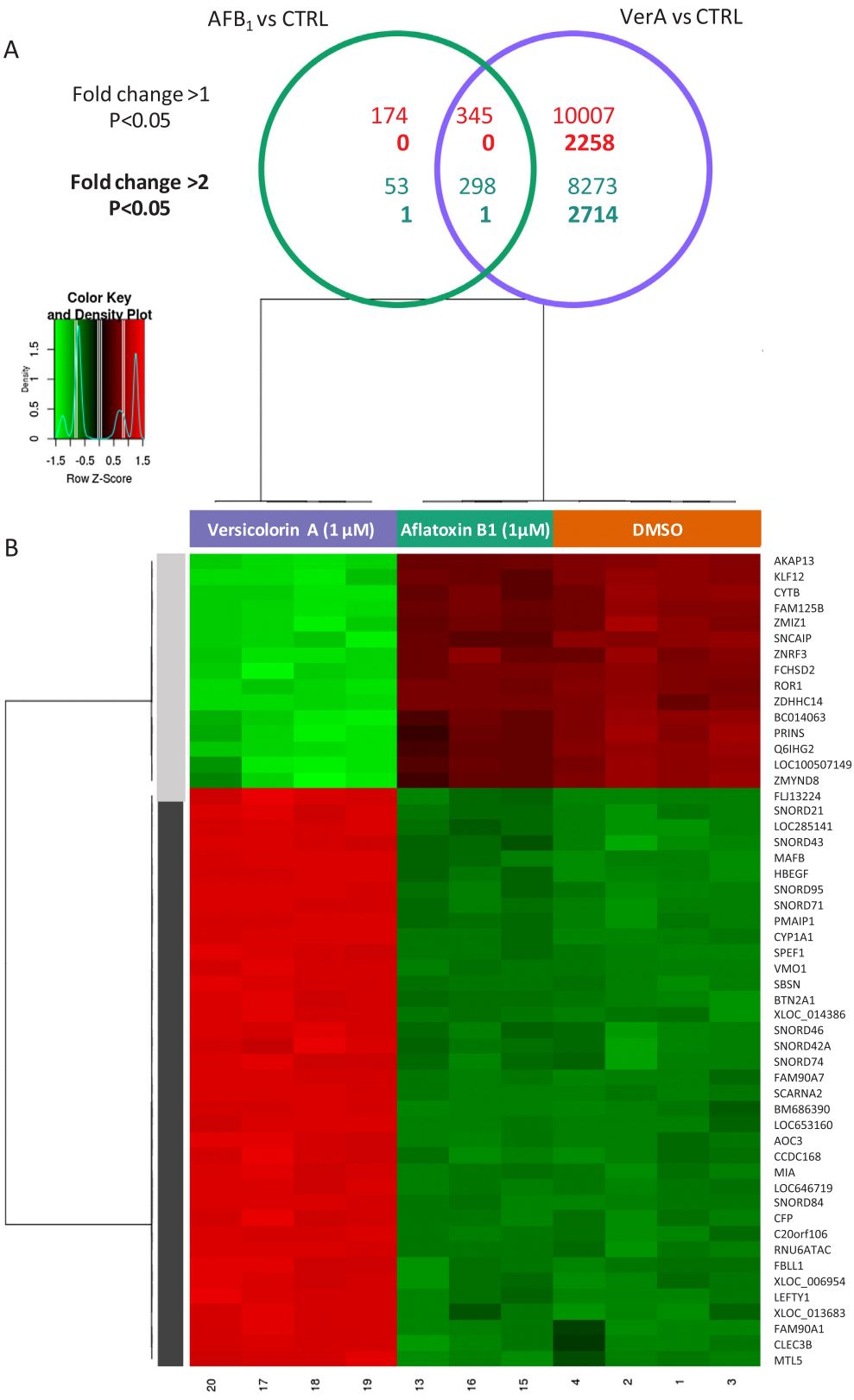

Fig. 10. Gene expression profile of Caco2 cell line exposed to 1 µM AFB_1 or VerA. Transcriptome analyses of the Caco2 cell line treated with AFB_1, VerA or DMSO (control) were performed using Agilent Sureprint G3 Human GE 8x60K microarray. Except for AFB_1 (n = 3), each group comprised four replicated cell cultures. 18 084 genes with FDR < 5% were considered significantly differently regulated in treated and DMSO cells. **A.** Venn diagram illustrating the overlaps between the genes significantly down- or up-regulated in response to AFB_1 and VerA treatment (adjusted P < 0.05). **B.** Expression profiles of genes displaying > 10-fold up- or down-regulation. Heatmap illustrates the gene expression profiles, and the hierarchical clustering was obtained from individual expression values using 1-Pearson correlation coefficient as distance and Ward's criterion for agglomeration. Red and green indicate values above and below the mean averaged centered and scaled expression values (Z-score), respectively.

causes more DNA damage in Caco-2 cells than AFB_1.

To confirm the above result, DNA strand breaks were then directly observed in Caco-2 cells using an alkaline comet assay. Under our conditions, only 10 µM of VerA induced detectable DNA lesions, whereas AFB_1 did not (Fig. 9B). As both mycotoxins have been shown to generate oxidative stress, the Fpg-modified comet assay was performed to reveal modifications to the oxidative base (Collins et al., 2014). Ro 19-8022, a chemical agent generating 8-oxoguanine, was used as a positive control whose DNA damage could be observed only after Fpg treatment. Although 10 µM AFB_1 was found to significantly increase DNA oxidation, the same concentration of VerA had a four-fold greater effect. Moreover, even a ten-fold lower concentration of VerA had a

higher oxidative effect than did 10 μM AFB_1 (Fig. S3). The oxidative effect revealed by DNA Fpg-sensitive sites could be due to the formation of either 8-oxoguanine (as a consequence of ROS formation) or to the formation of an aflatoxin B_1-formamidopyrimidine (AFB_1-FAPY) adduct (Smela et al., 2002), that can be recognized by Fpg enzyme (Coste et al., 2008). Due to its similar chemical structure to AFB_1, VerA, could also lead to VerA-FAPY adducts, hence participating in the increase in DNA damage after Fpg treatment. These data confirmed that VerA exerts greater genotoxic stress in Caco-2 cells than AFB_1, and that it is at least partly dependent on ROS formation.

To further elucidate the consequences of the genotoxic activity of VerA and AFB_1 in Caco-2 cells, micronucleus formation was quantified. Only cells treated with 1 μM of VerA showed significantly more micronucleus than non-treated cells (Fig. 9D). These data suggest that VerA may induce more genetic instability in Caco-2 cells than AFB_1. In addition, exposure to 10 μM of both mycotoxins impeded micronucleus formation in daughter cells by blocking mitotic entry, which was more severe after exposure to VerA than after exposure to AFB_1 (Fig. 9C).

DNA damage-mediated cell cycle arrest is governed by two main pathways: the ATM-Chk2 axis responding to double-strand breaks (DSBs) and the ATR-Chk1 axis responding to replication stress (RS) (Shaltiel et al., 2015). To get more insight into the genotoxic mode of action of AFB_1 and VerA, we analyzed these two cellular responses at greater depth. First, immunofluorescence analyses were performed to compare H2AX phosphorylation, which can be induced by ATM or ATR, to 53BP1 recruitment, which is more specific to DSBs (de Feraudy et al., 2010; Vignard et al., 2013). While some cells showed both ɣH2AX and 53BP1 signals after AFB_1 or VerA, a subpopulation of ɣH2AX-positive cells were devoid of 53BP1 foci (Fig. 9E), suggesting that RS is an early response to the mycotoxins before DSB formation. To corroborate this assumption, we investigated activation of the ATM and ATR pathways through the phosphorylation of Chk2 and Chk1, respectively. After 8 h of exposure, a slight increase in pChk1 was detected with 1 or 10 μM of AFB_1, whereas Chk2 phosphorylation was still not clearly observable (Fig. 9F). In the same way, VerA induced Chk1 phosphorylation at 8 h that was dose-dependent and stronger than AFB_1, but only a few pChk2 was observed at the highest concentration. Both AFB_1 and VerA-dependent Chk2 phosphorylation were detectable after 16 h, demonstrating that ATR was activated before ATM. Taken together, these results indicate that VerA is able to induce greater genotoxic stress than AFB_1, generating a RS that may subsequently lead to DSB formation.

3.6. Transcriptomic analysis

In order to assess the effect of AFB_1 and VerA treatment on the entire Caco-2 cell transcriptome, a microarray analysis was performed after 24 h of exposure to AFB_1, VerA and DMSO (control). VerA treatment led to 10 352 over expressed genes (12 244 probes) and 8 571 down expressed genes (10 841 probes) (Fig. 10A). Among them, 52 genes were up (37) or down (15) regulated with a fold change (FC) equal to or higher than 10 (Fig. 10B). By contrast, 519 up expressed genes (571 probes) and 351 down expressed genes (376 probes) were detected when Caco-2 cells were treated with AFB_1 with only two differentially expressed genes with a FC ≥ 2 (Fig. 10A).

Numerous genes encoding proteins involved in transcription and translation processes were up regulated in response to VerA treatment with a FC ≥ 2 (Fig. 10A). Among the proteins involved in the transcription were elongation factors as TCEA1 (FC = 2.35), TCEB2 (FC = 2.17), and TCEB3 (FC = 2.07), PAPOLA (FC = 2.64) involved in the poly (A) tail synthesis, few RNA polymerase II proteins as POLR2A (FC = 2.11), POLR2H (FC = 2.66) and POLR2K (FC = 2.03). Other proteins involved in the nuclear export of spliced and unspliced mRNA were also up expressed as NXF1 (FC = 4.23), ALYREF (FC = 2.10), NXT2 (FC = 2.48), UPF3B (FC = 2.17).

Among up regulated DEG, 49 small nucleolar H/ACA RNA (SNORA) genes and 72 small nucleolar C/D box RNA (SNORD) were up regulated with a fold change exceeding two (Fig. S4A and S4B). Surprisingly, a limited number of SNORD and SNORA were down regulated. H/ACA box functions as guide RNAs to direct the pseudouridylation in various type of RNA, while C/D box RNAs target the methyl-transferase fibrillarin in order to 2′-OH-ribose methylate rRNA. Surprisingly, several components of the minor spliceosome involved in the noncanonical splicing were also up regulated. Among them were U11 (FC = 6.63), U12 (FC = 2.95), U4atac (FC = 4.86), U6atac (FC = 29.84) small nuclear RNA and SnRNP48 (U11-48 K) (FC = 2.23).

CYP1A1, a CYP450 known to catalyze the epoxidation of compounds with carcinogenic properties, notably AFB_1 in rabbit lung and liver (Androutsopoulos et al., 2009), was 14.5 fold up regulated in VerA treated cells but not in AFB_1 treated cells. CYP1A2, one of the key cytochromes p450 involved in the formation of *exo*-8,9-epoxide in the human liver was also up regulated with a weaker fold change (2.38). Apoptosis seemed to be induced by VerA through up regulation of notably Noxa (PMAIP1) (28.3-fold increase) and Gadd45b (7.3-fold increase) genes, two pro-apoptotic factors. Data also showed that VerA can promote an inflammatory response mediated by up regulation of interleukins and induce a process leading to alteration of chromatid cohesion.

By contrast, microarray analysis showed that 24 genes located in the histone 1 gene cluster were down expressed (Fig. S4C) and that VerA seemed to affect the mitochondrial oxidative phosphorylation through down regulation of genes coding for enzymes of the respiratory chain.

4. Discussion

AFB_1 is a highly toxic mycotoxin frequently found in foodstuffs. However, our data (see Results in Supplementary Material, Table S3 and Fig. S5) showed that one of its metabolite intermediates, VerA, may be concomitantly present at rates exceeding the maximum level of AFB_1 established by the European Union in many cases: 2 μg/kg in peanuts, 5 μg/kg in corn and nuts, 8 μg/kg in almond and pistachio (European Parliament Commission Regulation, 2006). A recent study on commercial corn grain showed that accumulation of VerA at the beginning of storage followed by a decrease is predictive of future AFB_1 production (Zhang et al., 2018). Thus, depending on the length of storage, AFB_1 negative stocks could contain large amounts of VerA. Furthermore, the molecular structures of AFB_1 and VerA share a common backbone, making VerA potentially toxic for human health. Indeed, previous works reported that VerA was genotoxic for mouse and rat hepatocytes at doses as low as 5 μM (Mori et al., 1984) and more recently VerA was found to be genotoxic for human HepG2 hepatoblastoma cells and human LS-174 T colorectal adenocarcinoma intestinal cells at a dose of 1 μM (Theumer et al., 2018). However, no study had previously been conducted to compare the cytotoxicity process of AFB_1 and its precursor VerA in human intestinal cells.

First, the global transcriptomic approach showed that a larger number of genes were dysregulated when Caco-2 cells were exposed to VerA than in cells treated with AFB_1 (18 002 genes versus 869, respectively). This huge difference in the transcriptome response argued for higher potent cytotoxic effects of VerA compared to AFB_1. Indeed, we found that VerA induced higher oxidative stress, caused more DNA damage, stronger inhibition of cell proliferation and apoptotic cell death than observed after exposure to AFB_1. It is well known that ROS can cause DNA damage, which could result in cell cycle arrest and apoptotic cell death. In addition, previous studies have established that the reactive product of AFB_1, AFB_1-8,9- epoxide, is able to form DNA adducts that lead to DNA strand breaks. Both VerA and AFB_1 have a double bond in the same position in the terminal furan ring (12,13 in VerA and 15,16 in AFB_1), the latter being the site of activation of AFB_1 by the CYP450 family. In human liver, mainly CYP1A2 and CYP3A4 are involved in the bio activation of AFB_1 (Gallagher et al., 1994; Guengerich et al., 1998; Kim et al., 2016). However, CYP1A1 is an extrahepatic CYP450 able to catalyze the epoxidation of AFB_1

(Androutsopoulos et al., 2009). Interestingly, the transcriptomic analysis revealed that VerA but not AFB_1 induced a 14.5-fold expression of CYP1A1 in Caco-2 cells, suggesting that bioactivation of VerA could be achieved through this CYP450. This hypothesis is strengthened by previous results dealing with sterigmatocystin, the penultimate stable precursor of AFB_1 (Cabaret et al., 2010). Indeed, these results showed that: (i) sterigmatocystin, that also displays the double bond in the terminal furan ring, was transformed by CYP1A1; (ii) 1 μM sterigmatocystin induced an 18-fold increase of CYP1A1 transcripts level.

We also observed that AFB_1 could pass from the apical to the basolateral side of the Caco-2 cell layer whereas very few VerA was retrieved from the extra-cellular medium. These results support the hypothesis that, contrary to AFB_1, which could pass through the intestinal barrier, VerA could be converted to reactive compounds that have deleterious effects. Additional *in vitro* and *in vivo* studies are needed to confirm our hypothesis and to identify possible newly formed products resulting from VerA biotransformation.

Our results indicated that VerA had a stronger cytotoxic effect than AFB_1, decreasing cell proliferation and triggering an apoptotic process. Indeed, exposure to VerA slowed down the growth rate and increased apoptotic dead cells from a dose of 1 μM in Caco-2 cells. In response to DNA damage, the tumor suppressor p53 is known to mediate cell cycle arrest (Pucci et al., 2000) and apoptosis (Shamas-Din et al., 2011) and to be implicated in the regulation of the DNA repair pathway (Saha et al., 2015; Williams and Schumacher, 2016). Since it has previously been reported that the p53 gene in Caco-2 cells has deleted and mutated alleles and that no p53 protein is detectable in these cells (Djelloul et al., 1997; Liu and Bodmer, 2006), this pathway cannot be involved in the cytotoxic effects induced in Caco-2 cells. However, a previous study reported that the apoptosis pathway in Caco-2 cells could be induced by activation of p73, a homolog of p53 (Ozaki and Nakagawara, 2005), leading to the expression of apoptotic PUMA, Noxa and Siva-1 (Ray et al., 2011). Strikingly, our transcriptomic analysis revealed that Noxa was 28-fold over-expressed after exposure to VerA but not after exposure to AFB_1. Noxa is a sensitizer pro-apoptotic protein that binds to Mcl-1 and A1 anti-apoptotic proteins, thus promoting the apoptosis mitochondrial pathway (Oda et al., 2000; Shamas-Din et al., 2011) leading to a caspases cascade. Our results also showed that the genotoxic process induced by VerA involved a higher level of pChk2 than observed with AFB_1. This checkpoint kinase is known to regulate the pro-apoptotic factor E2F-1 (Stevens et al., 2003). Thus, this pathway could also be involved in the apoptotic cell death process induced by VerA.

The aim of using p53-/- and p53 wild-type HCT116 cells was to highlight the role of p53 in the cytotoxic process induced by VerA. Exposure to VerA induced phosphorylation of p53 in wild-type HCT116 cells, which was related to a slightly higher apoptotic response and a slightly more pronounced slowdown of the growth rate compared to p53 -/- HCT116 cells, arguing for a minor role of the p53 pathway in the VerA induced cytotoxicity. In addition, AFB_1 was capable of inducing even higher p53 activation than VerA with no cytotoxic effect. Similarly, a previous study on colon HCT-8 cells showed that AFB_1 caused a S-phase cell cycle arrest but no apoptosis and that this effect was partially under the control of p53 (Kim et al., 2016).

The inhibition of Caco-2 cell proliferation by VerA and AFB_1 was linked to reduced replication of dividing cells that led to the accumulation of S-phase cells at low concentrations (1 μM), however, the accumulation was offset by the initiation of apoptotic cell death at 5 μM VerA. Conversely, in HCT116 cells, the inhibition of cell proliferation by VerA was correlated with a decrease in S-phase cells and a drastic reduction in their replication. Although AFB_1 did not impair HCT116 cell proliferation, it significantly reduced the replication of S-cells but to a much lesser extent than when triggered by VerA. Concomitantly, AFB_1 triggered the accumulation of G2/M phase cells and S-phase cells in wild-type and p53 -/- HCT116 cells, respectively. These data are consistent with results obtained on jejunal cells of chicken fed with AFB_1 where the treatment induced a G2/M cell cycle arrest associated with increased p53 content (Yin et al., 2016). Obviously, these effects on the HCT116 cell cycle were not sufficient to have an adverse impact on the proliferation rate.

5. Conclusions

Altogether, our results demonstrate that VerA has a stronger genotoxic and cytotoxic effect than AFB_1 on intestinal cell lines. Exposure to low concentrations of VerA (1–20 μM) leads to the inhibition of cell proliferation and to cell death. Moreover, VerA exposure leads to the dysregulation of thousands of genes, highlighting the strong impact of this mycotoxin. The presence of VerA in food commodities such as corn, groundnuts and nuts from many different countries raises questions about its threat for human health.

Further, since VerA and AFB_1 may contaminate foodstuff concomitantly, another study should investigate the combined effect of these two mycotoxins.

CRediT authorship contribution statement

Thierry Gauthier: Conceptualization, Investigation, Writing - original draft. **Carolina Duarte-Hospital:** Methodology, Investigation. **Julien Vignard:** Investigation, Writing - original draft. **Elisa Boutet-Robinet:** Investigation, Writing - original draft. **Michael Sulyok:** Investigation, Writing - original draft. **Selma P. Snini:** Methodology, Investigation. **Imourana Alassane-Kpembi:** Investigation. **Yannick Lippi:** Formal analysis, Writing - original draft. **Sylvie Puel:** Methodology, Investigation. **Isabelle P. Oswald:** Funding acquisition, Supervision. **Olivier Puel:** Conceptualization, Writing - original draft.

Declaration of Competing Interest

The authors declare that they have no known competing financial interests or personal relationships that could have appeared to influence the work reported in this paper.

Acknowledgments

We would like to thank Joelle Laffitte, Souria Tadrist and Adeline Saysset for their excellent technical assistance and Dr Bert Vogelstein for providing the HCT116 cell lines. We are very grateful to Dr Laurence Huc for her valuable advices along this study. This research was funded by the ANR (Agence Nationale de la Recherche) under Grant ANR-11-ALID-0003 AFLAFREE and by CAPES-COFECUB (Coordenação de Aperfeiçoamento de Pessoal de Nível Superior - Comité Français d'Evaluation de la Coopération Universitaire et scientifique avec le Brésil) under grant SV 947/19. We also thank Mrs Daphne Goodfellow for her editing of this document.

Appendix A. Supplementary data

Supplementary data to this article can be found online at https://doi.org/10.1016/j.envint.2020.105568.

References

Androutsopoulos, V.P., Tsatsakis, A.M., Spandidos, D.A., 2009. Cytochrome P450 CYP1A1: wider roles in cancer progression and prevention. BMC Cancer 9, 187. https://doi.org/10.1186/1471-2407-9-187.

Azqueta, A., Arbillaga, L., López de Cerain, A., Collins, A., 2013. Enhancing the sensitivity of the comet assay as a genotoxicity test, by combining it with bacterial repair enzyme FPG. Mutagenesis 28, 271–277. https://doi.org/10.1093/mutage/get002.

Bailly, S., Mahgubi, A.E., Carvajal-Campos, A., Lorber, S., Puel, O., Oswald, I.P., Bailly, J.-D., Orlando, B., 2018. Occurrence and identification of *Aspergillus* section *Flavi* in the context of the emergence of Aflatoxins in French Maize. Toxins 10, E525. https://doi.org/10.3390/toxins10120525.

Battilani, P., Toscano, P., Van der Fels-Klerx, H.J., Moretti, A., Camardo Leggieri, M.,

Brera, C., Rortais, A., Goumperis, T., Robinson, T., 2016. Aflatoxin B1 contamination in maize in Europe increases due to climate change. Sci. Rep. 6, 24328. https://doi.org/10.1038/srep24328.
Benjamini, H., Hochberg, Y., 1995. Controlling the False Discovery Rate: a practical and powerful approach to multiple testing. J. R. Stat. Soc 57, 289–300.
Bennett, R.A., Essigmann, J.M., Wogan, G.N., 1981. Excretion of an aflatoxin-guanine adduct in the urine of aflatoxin B1-treated rats. Cancer Res. 41, 650–654.
Bianco, G., Russo, R., Marzocco, S., Velotto, S., Autore, G., Severino, L., 2012. Modulation of macrophage activity by aflatoxins B1 and B2 and their metabolites aflatoxins M1 and M2. Toxicon 59, 644–650. https://doi.org/10.1016/j.toxicon.2012.02.010.
Cabaret, O., Puel, O., Botterel, F., Pean, M., Khoufache, K., Costa, J.-M., Delaforge, M., Bretagne, S., 2010. Metabolic detoxication pathways for sterigmatocystin in primary tracheal epithelial cells. Chem. Res. Toxicol. 23, 1673–1681. https://doi.org/10.1021/tx100127b.
Cano, P., Puel, O., Oswald, I.P., 2016. Mycotoxins: fungal secondary metabolites with toxic properties. In: Misra, J., Tewari, J., Papp, T. (Eds.), Fungi. Applications and Management Strategies. CRC Press, pp. 318–371.
Collins, A.R., El Yamani, N., Lorenzo, Y., Shaposhnikov, S., Brunborg, G., Azqueta, A., 2014. Controlling variation in the comet assay. Front. Genet. 5, 359. https://doi.org/10.3389/fgene.2014.00359.
Cook, P.J., Ju, B.G., Telese, F., Wang, X., Glass, C.K., Rosenfeld, M.G., 2009. Tyrosine dephosphorylation of H2AX modulates apoptosis and survival decisions. Nature 458, 591–596. https://doi.org/10.1038/nature07849.
Coste, F., Ober, M., Le Bihan, Y.-V., Izquierdo, M.A., Hervouet, N., Mueller, H., Carell, T., Castaing, B., 2008. Bacterial base excision repair enzyme Fpg recognizes bulky N7-substituted-FapydG lesion via unproductive binding mode. Chem. Biol. 15, 706–717. https://doi.org/10.1016/j.chembiol.2008.05.014.
de Feraudy, S., Revet, I., Bezrookove, V., Feeney, L., Cleaver, J.E., 2010. A minority of foci or pan-nuclear apoptotic staining of gammaH2AX in the S phase after UV damage contain DNA double-strand breaks. Proc. Natl. Acad. Sci. U.S.A. 107, 6870–6875. https://doi.org/10.1073/pnas.1002175107.
Djelloul, S., Forgue-Lafitte, M.E., Hermelin, B., Mareel, M., Bruyneel, E., Baldi, A., Giordano, A., Chastre, E., Gespach, C., 1997. Enterocyte differentiation is compatible with SV40 large T expression and loss of p53 function in human colonic Caco-2 cells. Status of the pRb1 and pRb2 tumor suppressor gene products. FEBS Lett. 406, 234–242.
European Parliament Commission Regulation, 2006. Setting maximum levels for certain contaminants in foodstuffs. J. Eur. Union L364, 1–28.
Gallagher, E.P., Wienkers, L.C., Stapleton, P.L., Kunze, K.L., Eaton, D.L., 1994. Role of human microsomal and human complementary DNA-expressed cytochromes P4501A2 and P4503A4 in the bioactivation of aflatoxin B1. Cancer Res. 54, 101–108.
Gauthier, T., Wang, X., Sifuentes Dos Santos, J., Fysikopoulos, A., Tadrist, S., Canlet, C., Artigot, M.P., Loiseau, N., Oswald, I.P., Puel, O., 2012. Trypacidin, a spore-borne toxin from *Aspergillus fumigatus*, is cytotoxic to lung cells. PLoS ONE 7, e29906. https://doi.org/10.1371/journal.pone.0029906.
Ge, J., Yu, H., Li, J., Lian, Z., Zhang, H., Fang, H., Qian, L., 2017. Assessment of aflatoxin B1 myocardial toxicity in rats: mitochondrial damage and cellular apoptosis in cardiomyocytes induced by aflatoxin B1. J. Int. Med. Res. 45, 1015–1023. https://doi.org/10.1177/0300060517706579.
Guengerich, F.P., Johnson, W.W., Shimada, T., Ueng, Y.F., Yamazaki, H., Langouët, S., 1998. Activation and detoxication of aflatoxin B1. Mutat. Res. 402, 121–128.
Huber, W., Carey, V.J., Gentleman, R., Anders, S., Carlson, M., Carvalho, B.S., Bravo, H.C., Davis, S., Gatto, L., Girke, T., Gottardo, R., Hahne, F., Hansen, K.D., Irizarry, R.A., Lawrence, M., Love, M.I., MacDonald, J., Obenchain, V., Oleś, A.K., Pagès, H., Reyes, A., Shannon, P., Smyth, G.K., Tenenbaum, D., Waldron, L., Morgan, M., 2015. Orchestrating high-throughput genomic analysis with Bioconductor. Nat. Methods 12, 115–121. https://doi.org/10.1038/nmeth.3252.
International Agency for Research on Cancer, Weltgesundheitsorganisation (Eds.), 2012. IARC monographs on the evaluation of carcinogenic risks to humans, volume 100 F, chemical agents and related occupations: this publication represents the views and expert opinions of an IARC Working Group on the Evaluation of Carcinogenic Risks to Humans, which met in Lyon, 20 - 27 October 2009. IARC, Lyon.
Jakšić, D., Puel, O., Canlet, C., Kopjar, N., Kosalec, I., Klarić, M.Š., 2012. Cytotoxicity and genotoxicity of versicolorins and 5-methoxysterigmatocystin in A549 cells. Arch. Toxicol. 86, 1583–1591. https://doi.org/10.1007/s00204-012-0871-x.
Kew, M.C., 2013. Aflatoxins as a cause of hepatocellular carcinoma. J. Gastrointest. Liver Dis. 22, 305–310.
Kim, B.M., Rode, A.B., Han, E.J., Hong, I.S., Hong, S.H., 2012. 5-Phenylselenyl- and 5-methylselenyl-methyl-2′-deoxyuridine induce oxidative stress, DNA damage, and caspase-2-dependent apoptosis in cancer cells. Apoptosis 17, 200–216. https://doi.org/10.1007/s10495-011-0665-2.
Kim, J., Park, S.-H., Do, K.H., Kim, D., Moon, Y., 2016. Interference with mutagenic aflatoxin B1-induced checkpoints through antagonistic action of ochratoxin A in intestinal cancer cells: a molecular explanation on potential risk of crosstalk between carcinogens. Oncotarget 7, 39627–39639. https://doi.org/10.18632/oncotarget.8914.
Lee, L.S., Bennett, J.W., Cucullu, A.F., Ory, R.L., 1976. Biosynthesis of aflatoxin B1. Conversion of versicolorin A to aflatoxin B1 by *Aspergillus parasiticus*. J. Agric. Food Chem. 24, 1167–1170.
Liao, S., Shi, D., Clemons-Chevis, C.L., Guo, S., Su, R., Qiang, P., Tang, Z., 2014. Protective role of selenium on aflatoxin B1-induced hepatic dysfunction and apoptosis of liver in ducklings. Biol. Trace Elem. Res. 162, 296–301. https://doi.org/10.1007/s12011-014-0131-4.
Liu, Y., Bodmer, W.F., 2006. Analysis of P53 mutations and their expression in 56 colorectal cancer cell lines. Proc. Natl. Acad. Sci. U. S. A. 103, 976–981. https://doi.org/10.1073/pnas.0510146103.
Liu, Y., Wang, W., 2016. Aflatoxin B1 impairs mitochondrial functions, activates ROS generation, induces apoptosis and involves Nrf2 signal pathway in primary broiler hepatocytes. Anim. Sci. J. 87, 1490–1500. https://doi.org/10.1111/asj.12550.
Mori, H., Kawai, K., Ohbayashi, F., Kuniyasu, T., Yamazaki, M., Hamasaki, T., Williams, G.M., 1984. Genotoxicity of a variety of mycotoxins in the hepatocyte primary culture/DNA repair test using rat and mouse hepatocytes. Cancer Res. 44, 2918–2923.
Mori, H., Kitamura, J., Sugie, S., Kawai, K., Hamasaki, T., 1985. Genotoxicity of fungal metabolites related to aflatoxin B1 biosynthesis. Mutat. Res. 143, 121–125.
Oda, E., Ohki, R., Murasawa, H., Nemoto, J., Shibue, T., Yamashita, T., Tokino, T., Taniguchi, T., Tanaka, N., 2000. Noxa, a BH3-Only Member of the Bcl-2 Family and Candidate Mediator of p53-Induced Apoptosis. Science 288, 1053–1058. https://doi.org/10.1126/science.288.5468.1053.
Ozaki, T., Nakagawara, A., 2005. p73, a sophisticated p53 family member in the cancer world. Cancer Sci. 96, 729–737. https://doi.org/10.1111/j.1349-7006.2005.00116.x.
Peng, X., Yu, Z., Liang, N., Chi, X., Li, X., Jiang, M., Fang, J., Cui, H., Lai, W., Zhou, Y., Zhou, S., 2016. The mitochondrial and death receptor pathways involved in the thymocytes apoptosis induced by aflatoxin B1. Oncotarget 7, 12222–12234. https://doi.org/10.18632/oncotarget.7731.
Perdry, H., Gutzkow, K.B., Chevalier, M., Huc, L., Brunborg, G., Boutet-Robinet, E., 2018. Validation of Gelbond® high-throughput alkaline and Fpg-modified comet assay using a linear mixed model. Environ. Mol. Mutagen. 59, 595–602. https://doi.org/10.1002/em.22204.
Pinton, P., Tsybulskyy, D., Lucioli, J., Laffitte, J., Callu, P., Lyazhri, F., Grosjean, F., Bracarense, A.P., Kolf-Clauw, M., Oswald, I.P., 2012. Toxicity of deoxynivalenol and its acetylated derivatives on the intestine: differential effects on morphology, barrier function, tight junction proteins, and mitogen-activated protein kinases. Toxicol. Sci. 130, 180–190. https://doi.org/10.1093/toxsci/kfs239.
Podhorecka, M., Skladanowski, A., Bozko, P., 2010. H2AX Phosphorylation: Its Role in DNA Damage Response and Cancer Therapy. J. Nucleic Acids, pii:920161. https://doi.org/10.4061/2010/920161.
Pucci, B., Kasten, M., Giordano, A., 2000. Cell cycle and apoptosis. Neoplasia N. Y. N 2, 291–299.
R Core Team, 2018. R: A language and environment for statistical computing. R Foundation for Statistical Computing, Vienna, Austria.
Ray, R.M., Bhattacharya, S., Johnson, L.R., 2011. Mdm2 inhibition induces apoptosis in p53 deficient human colon cancer cells by activating p73- and E2F1-mediated expression of PUMA and Siva-1. Apoptosis 16, 35–44. https://doi.org/10.1007/s10495-010-0538-0.
Ritchie, M.E., Phipson, B., Wu, D., Hu, Y., Law, C.W., Shi, W., Smyth, G.K., 2015. limma powers differential expression analyses for RNA-sequencing and microarray studies. Nucleic Acids Res. 43, e47. https://doi.org/10.1093/nar/gkv007.
Saha, T., Kar, R.K., Sa, G., 2015. Structural and sequential context of p53: A review of experimental and theoretical evidence. Prog. Biophys. Mol. Biol. 117, 250–263. https://doi.org/10.1016/j.pbiomolbio.2014.12.002.
Shaltiel, I.A., Krenning, L., Bruinsma, W., Medema, R.H., 2015. The same, only different - DNA damage checkpoints and their reversal throughout the cell cycle. J. Cell Sci. 128, 607–620. https://doi.org/10.1242/jcs.163766.
Shamas-Din, A., Brahmbhatt, H., Leber, B., Andrews, D.W., 2011. BH3-only proteins: Orchestrators of apoptosis. Biochim. Biophys. Acta 1813, 508–520. https://doi.org/10.1016/j.bbamcr.2010.11.024.
Smela, M.E., Hamm, M.L., Henderson, P.T., Harris, C.M., Harris, T.M., Essigmann, J.M., 2002. The aflatoxin B(1) formamidopyrimidine adduct plays a major role in causing the types of mutations observed in human hepatocellular carcinoma. Proc. Natl. Acad. Sci. U. S. A. 99, 6655–6660. https://doi.org/10.1073/pnas.102167699.
Smyth, G.K., 2004. Linear models and empirical bayes methods for assessing differential expression in microarray experiments. Stat. Appl. Genet. Mol. Biol. 3https://doi.org/10.2202/1544-6115.1027. Article3.
Speidel, D., 2015. The role of DNA damage responses in p53 biology. Arch. Toxicol. 89, 501–517. https://doi.org/10.1007/s00204-015-1459-z.
Stevens, C., Smith, L., La Thangue, N.B., 2003. Chk2 activates E2F–1 in response to DNA damage. Nat. Cell Biol. 5, 401–409. https://doi.org/10.1038/ncb974.
Strosnider, H., Azziz-Baumgartner, E., Banziger, M., Bhat, R.V., Breiman, R., Brune, M.-N., DeCock, K., Dilley, A., Groopman, J., Hell, K., Henry, S.H., Jeffers, D., Jolly, C., Jolly, P., Kibata, G.N., Lewis, L., Liu, X., Luber, G., McCoy, L., Mensah, P., Miraglia, M., Misore, A., Njapau, H., Ong, C.-N., Onsongo, M.T.K., Page, S.W., Park, D., Patel, M., Phillips, T., Pineiro, M., Pronczuk, J., Rogers, H.S., Rubin, C., Sabino, M., Schaafsma, A., Shephard, G., Stroka, J., Wild, C., Williams, J.T., Wilson, D., 2006. Workgroup report: public health strategies for reducing aflatoxin exposure in developing countries. Environ. Health Perspect. 114, 1898–1903. https://doi.org/10.1289/ehp.9302.
Tannous, J., Snini, S.P., El Khoury, R., Canlet, C., Pinton, P., Lippi, Y., Alassane-Kpembi, I., Gauthier, T., El Khoury, A., Atoui, A., Zhou, T., Lteif, R., Oswald, I.P., Puel, O., 2017. Patulin transformation products and last intermediates in its biosynthetic pathway, E- and Z-ascladiol, are not toxic to human cells. Arch. Toxicol. 91, 2455–2467. https://doi.org/10.1007/s00204-016-1900-y.
Thannickal, V.J., Fanburg, B.L., 2000. Reactive oxygen species in cell signaling. Am. J. Physiol.-Lung Cell. Mol. Physiol. 279, 1005–1028. https://doi.org/10.1152/ajplung.2000.279.6.L1005.
Theumer, M.G., Henneb, Y., Khoury, L., Snini, S.P., Tadrist, S., Canlet, C., Puel, O., Oswald, I.P., Audebert, M., 2018. Genotoxicity of aflatoxins and their precursors in human cells. Toxicol. Lett. 287, 100–107. https://doi.org/10.1016/j.toxlet.2018.02.007.
Vignard, J., Mirey, G., Salles, B., 2013. Ionizing-radiation induced DNA double-strand breaks: a direct and indirect lighting up. Radiother. Oncol. 108, 362–369. https://doi.org/10.1016/j.radonc.2013.06.013.

Vousden, K.H., Prives, C., 2009. Blinded by the Light: the growing complexity of p53. Cell 137, 413–431. https://doi.org/10.1016/j.cell.2009.04.037.

Williams, A.B., Schumacher, B., 2016. p53 in the DNA-damage-repair process. Cold Spring Harb. Perspect. Med. 6https://doi.org/10.1101/cshperspect.a026070. Pii: a026070.

Williams, J.H., Phillips, T.D., Jolly, P.E., Stiles, J.K., Jolly, C.M., Aggarwal, D., 2004. Human aflatoxicosis in developing countries: a review of toxicology, exposure, potential health consequences, and interventions. Am. J. Clin. Nutr. 80, 1106–1122. https://doi.org/10.1093/ajcn/80.5.1106.

Yang, X., Lv, Y., Huang, K., Luo, Y., Xu, W., 2016. Zinc inhibits aflatoxin B1-induced cytotoxicity and genotoxicity in human hepatocytes (HepG2 cells). Food Chem. Toxicol. 92, 17–25. https://doi.org/10.1016/j.fct.2016.03.012.

Yin, H., Jiang, M., Peng, X., Cui, H., Zhou, Y., He, M., Zuo, Z., Ouyang, P., Fan, J., Fang, J., 2016. The molecular mechanism of G2M cell cycle arrest induced by AFB1 in the jejunum. Oncotarget 7, 35592–35606. https://doi.org/10.18632/oncotarget.9594.

Yuan, S., Wu, B., Yu, Z., Fang, J., Liang, N., Zhou, M., Huang, C., Peng, X., 2016. The mitochondrial and endoplasmic reticulum pathways involved in the apoptosis of bursa of Fabricius cells in broilers exposed to dietary aflatoxin B 1. Oncotarget 7, 65295–65306. https://doi.org/10.18632/oncotarget.11321.

Zhang, M., Harashima, N., Moritani, T., Huang, W., Harada, M., 2015b. The Roles of ROS and Caspases in TRAIL-induced apoptosis and necroptosis in human pancreatic cancer cells. PLoS ONE 10. https://doi.org/10.1371/journal.pone.0127386.

Zhang, S.-Y., Wang, H., Yang, M., Yao, D.-S., Xie, C.-F., Liu, D.-L., 2018. Versicolorin A is a potential indicator of aflatoxin contamination in the granary-stored corn. Food Addit. Contam. Part Chem. Anal. Control Expo. Risk Assess. 35, 972–984. https://doi.org/10.1080/19440049.2017.1419579.

Zhang, J., Zheng, N., Liu, J., Li, F.D., Li, S.L., Wang, J.Q., 2015a. Aflatoxin B1 and aflatoxin M1 induced cytotoxicity and DNA damage in differentiated and undifferentiated Caco-2 cells. Food Chem. Toxicol. 83, 54–60. https://doi.org/10.1016/j.fct.2015.05.020.

Zhu, P., Zuo, Z., Zheng, Z., Wang, F., Peng, X., Fang, J., Cui, H., Gao, C., Song, H., Zhou, Y., Liu, X., 2017. Aflatoxin B1 affects apoptosis and expression of death receptor and endoplasmic reticulum molecules in chicken spleen. Oncotarget 8, 99531–99540. https://doi.org/10.18632/oncotarget.20595.